GGA1 regulates signal-dependent sorting of BACE1 to recycling endosomes, which moderates Aβ production

Wei Hong Toh, Pei Zhi Cheryl Chia†, Mohammed Iqbal Hossain, and Paul A. Gleeson*
Department of Biochemistry and Molecular Biology and Bio21 Molecular Science and Biotechnology Institute, The University of Melbourne, Melbourne, Victoria 3010, Australia

ABSTRACT **The diversion of the membrane-bound β-site amyloid precursor protein–(APP) cleaving enzyme (BACE1) from the endolysosomal pathway to recycling endosomes represents an important transport step in the regulation of amyloid beta (Aβ) production. However, the mechanisms that regulate endosome sorting of BACE1 are poorly understood. Here we assessed the transport of BACE1 from early to recycling endosomes and have identified essential roles for the sorting nexin 4 (SNX4)-mediated, signal-independent pathway and for a novel signal-mediated pathway. The signal-mediated pathway is regulated by the phosphorylation of the DXXLL-motif sequence DISLL in the cytoplasmic tail of BACE1. The phosphomimetic S498D BACE1 mutant was trafficked to recycling endosomes at a faster rate compared with wild-type BACE1 or the nonphosphorylatable S498A mutant. The rapid transit of BACE1 S498D from early endosomes was coupled with reduced levels of amyloid precursor protein processing and Aβ production, compared with the S498A mutant. We show that the adaptor, GGA1, and retromer are essential to mediate rapid trafficking of phosphorylated BACE1 to recycling endosomes. In addition, the BACE1 DISLL motif is phosphorylated and regulates endosomal trafficking, in primary neurons. Therefore, post-translational phosphorylation of DISLL enhances the exit of BACE1 from early endosomes, a pathway mediated by GGA1 and retromer, which is important in regulating Aβ production.**

Monitoring Editor
Jean E. Gruenberg
University of Geneva

Received: May 2, 2017
Revised: Oct 16, 2017
Accepted: Nov 8, 2017

INTRODUCTION

Membrane proteins from the plasma membrane (PM) of mammalian cells are endocytosed by a number of different routes involving both clathrin- and non–clathrin-mediated pathways that then all converge on early endosomes (Grant and Donaldson, 2009; Rajendran *et al.*, 2010). At the early endosomes membrane cargoes are sorted into a variety of different intracellular trafficking pathways, including transport from the early endosomes to the late endosomes/lysosomes for degradation, to the *trans*-Golgi network (TGN), or recycling back to the PM. Recycling to the PM can involve a fast route directly from the early endosomes back to the cell surface or indirectly via the recycling endosomes (Hsu and Prekeris, 2010; Hsu *et al.*, 2012), or the TGN (Lieu and Gleeson, 2011), both located deeper in the perinuclear region of the cell. Recycling of membrane cargo is relevant for a variety of cellular processes, including signaling, nutrient uptake, cell–cell adhesion, and cell development (van Ijzendoorn, 2006), and recycling of the membrane proteins provides a mechanism to regulate these activities. Endosomal sorting involves the partitioning of membrane cargo into membrane tubules that emanate from the body of the endosome and subsequently pinch off to form discrete transport carriers. Various machinery components are required to facilitate cargo sorting and to induce tubulation, such as sorting nexins (Gallon and Cullen, 2015), the coat complex retromer,

This article was published online ahead of print in MBoC in Press (http://www.molbiolcell.org/cgi/doi/10.1091/mbc.E17-05-0270) on November 15, 2017.
The authors declare no competing financial interests.
Author contributions: Experiments were designed by W.H.T. and P.A.G. P.Z.C.C. generated BACE1 phosphomutants and stable CHO cell lines. M.I.H. provided expertise to prepare primary neuron cultures. The article was written by W.H.T. and P.A.G.

†Present address: Institute of Dental and Craniofacial Research, National Institutes of Health, Bethesda, MD 20892-2190.
*Address correspondence to: Paul Gleeson (pgleeson@unimelb.edu.au).

Abbreviations used: Aβ, beta-amyloid peptide; AD, Alzheimer's disease; APP, amyloid precursor protein; BACE1, β-site APP-cleaving enzyme; GGA, Golgi-localized γ-ear containing Arf binding proteins; M6P, mannose-6-phosphate; SNX, sorting nexin; TfR, transferrin receptor; TGN, *trans*-Golgi network.

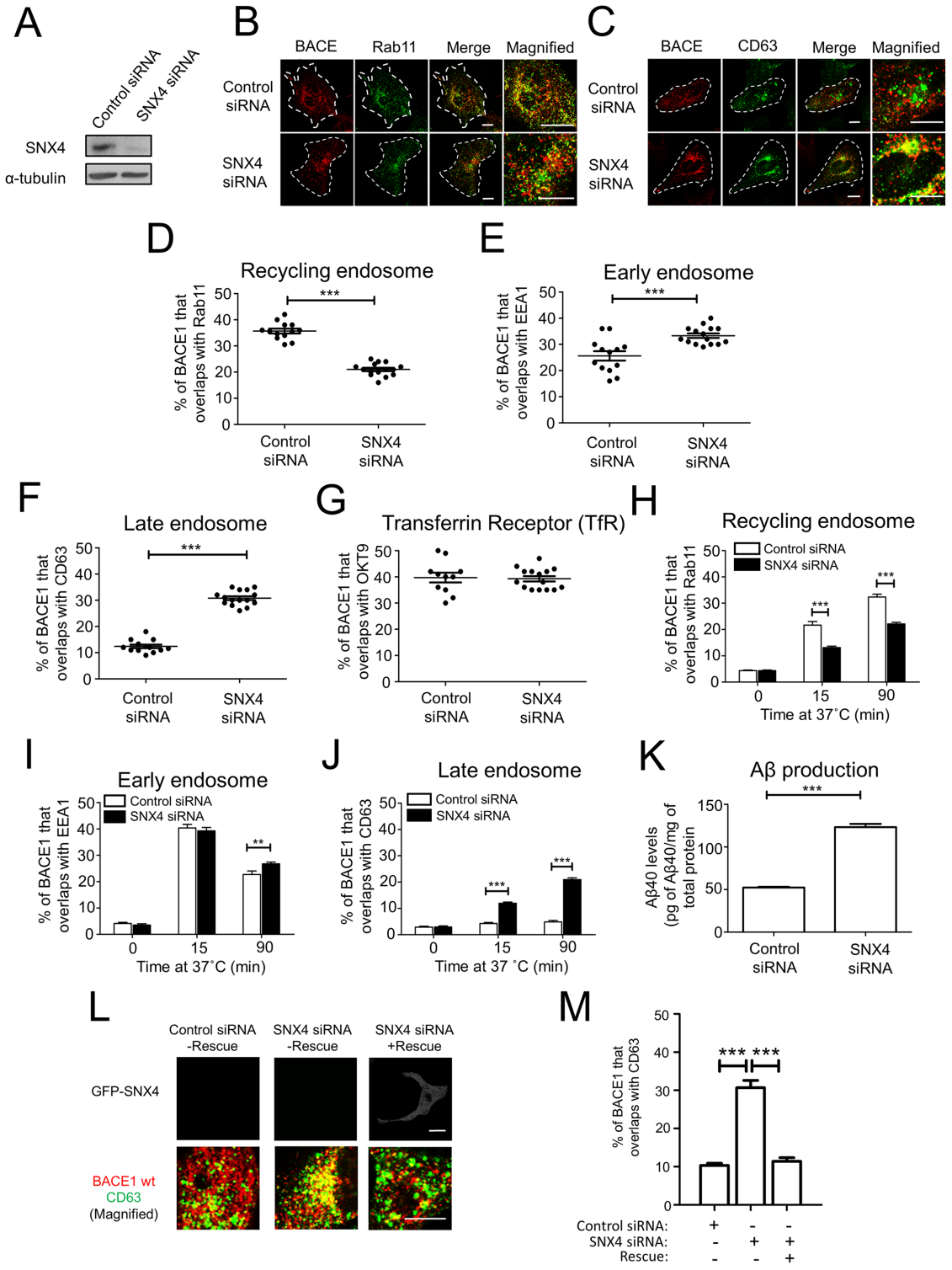

FIGURE 1: SNX4 depletion reduces BACE1 colocalization with Rab11. (A–M) HeLa cells were transfected with either control siRNA or SNX4 siRNA for 72 h and transfected with the wtBACE1 construct for a further 24 h. (A) Immunobloting of cell extracts with goat anti-SNX4 antibody and mouse anti–α-tubulin antibody, using a chemiluminescence detection system. (B, C) Confocal microscopic images of fixed and permeabilized monolayers stained with rabbit polyclonal anti-human BACE1 antibodies (red) and (B) mouse monoclonal antibodies to Rab11 (green) or (C) mouse monoclonal antibodies to CD63 (green). Higher magnifications of the merge images are shown. Bars represent 10 μm. (D–G) Percentage of BACE1 at the (D) recycling endosomes, (E) early endosomes, (F) late endosomes, and (G) with the transferrin receptor was calculated from the percentage of total BACE1 pixels that overlapped with Rab11, EEA1, CD63, or OKT9, respectively. Data from three independent experiments. (H–J) Internalization and trafficking of cell surface BACE1. Transfected cells were incubated with anti-BACE1 antibodies on ice for 30 min and unbound antibodies removed. Antibody-BACE1 complexes were internalized by shifting the

as well as additional cargo adaptor proteins (Popoff *et al.*, 2007; Seaman, 2007; Collins, 2008; Wassmer *et al.*, 2009; Cullen and Korswagen, 2012). Sorting nexins (SNXs) play important roles in the sorting of membrane cargo and/or promoting membrane curvature and tubulation. For example, SNX27, in collaboration with retromer, interacts with a number of sorting motifs for fast retrieval of cargo back to the cell surface (Balana *et al.*, 2011; Ghai *et al.*, 2013; Clairfeuille *et al.*, 2016), whereas SNX4 is considered to be primarily responsible for the generation of another class of transport carrier from the early endosome (Traer *et al.*, 2007). Retromer is a membrane coat protein complex that recruits cargoes such as the mannose-6-phosphate (M6P) receptor into transport carriers destined for the TGN (Seaman, 2007).

The events of endosomal sorting play a critical role in the regulation of proteolytic processing of the membrane-bound amyloid precursor protein (APP) by the β-site APP-cleaving enzyme BACE1 (Wang *et al.*, 2014; Peric and Annaert, 2015). BACE1 processing of APP is the rate-limiting step in the generation of pathogenic amyloid-beta (Aβ) peptides. Aβ peptides generated in endosomal compartments are released from the cell and aggregate to form deposits, which are the hallmark of senile plaques in Alzheimer's disease (AD) (Toh and Gleeson, 2016). The early endosome is considered a major intracellular compartment for the processing of APP and generation of Aβ (Kinoshita *et al.*, 2003; Rajendran *et al.*, 2006; Small and Gandy, 2006). Both APP and BACE1 are membrane proteins with sorting signals in their cytoplasmic tails. APP is directed along the lysosomal pathway from early endosomes (Koo *et al.*, 1996; Kinoshita *et al.*, 2003; Lorenzen *et al.*, 2010; Chia *et al.*, 2013; Das *et al.*, 2016; Toh *et al.*, 2016), whereas BACE1 is diverted from early endosomes to the recycling endosomes and then recycled to the PM (Buggia-Prevot *et al.*, 2013, 2014; Chia *et al.*, 2013; Das *et al.*, 2013; Udayar *et al.*, 2013). The trafficking of BACE1 from early endosomes is likely to be a critical step to segregate BACE1 from its substrate APP and potentially limit the extent of processing. An important consideration in understanding the regulation of APP processing is the efficiency of BACE1 transport from early endosomes. However, there is a paucity of information on the temporal events associated with endosomal sorting of BACE1. There is evidence that a deficiency of retromer impacts APP processing and Aβ production (Small *et al.*, 2005; Muhammad *et al.*, 2008; Sullivan *et al.*, 2011; Wen *et al.*, 2011; Mecozzi *et al.*, 2014); however, little is known about the machinery required for the transport of BACE1 selectively to the recycling endosomes. Indeed, the pathway from early endosomes to recycling endosomes has been considered in the field to be a signal-independent or default-pathway-mediated by SNX4-tubules that are continuously formed from the early endosomes (van Weering and Cullen, 2014). It remains unclear whether specific sorting signals contribute to cargo sorting from the early endosomes to recycling endosomes.

A number of sorting motifs in the cytoplasmic tail of BACE1 have been identified. The internalization of BACE1 from the PM is dependent on a dileucine motif (L499 and L500) (Huse *et al.*, 2000; Pastorino *et al.*, 2002; He *et al.*, 2005) which is part of an acidic cluster–dileucine motif (DXXLL), composed of DISLL residues. More recently, this DISLL sequence has been shown to be embedded within a longer [DE]XXX[LI]-motif sequence, namely DDISLL, and the first aspartate (Asp495) as well as the dileucine residues are required for AP2-mediated clathrin-dependent endocytosis of BACE1 from the PM (Prabhu *et al.*, 2012; Chia *et al.*, 2013).

Phosphorylation of Ser498 within the DISLL motif can also contribute to BACE1 trafficking (Walter *et al.*, 2001). Mutation of Ser498 to alanine resulted in the accumulation of BACE1 in the early endosomes, whereas mutation of Ser498 to an aspartic acid to mimic phosphorylated BACE1 was reported to result in BACE1 accumulating in the perinuclear region considered to be the TGN (Walter *et al.*, 2001; Pastorino *et al.*, 2002; He *et al.*, 2005). Although the TGN location of the latter mutant is difficult to reconcile with the current view of BACE1 recycling, these early studies clearly showed that phosphorylation of Ser498 influenced intracellular trafficking. In vitro binding studies have also showed that Golgi-localized γ-ear containing Arf binding proteins (GGA) proteins can interact with the DISLL motif (He *et al.*, 2005), an interaction that regulates intracellular transport. However, it is not known whether the interaction of BACE1 with GGA adaptors contribute to the sorting events in the early endosome.

Knowledge of the machinery and signals required for BACE1 sorting in the early endosome is critical for understanding the convergence of BACE1 with APP in this compartment and subsequent APP processing and Aβ production. Here we have investigated the roles of SNX4, retromer, and GGA1 in trafficking of BACE1 to the recycling endosomes. We demonstrate that the phosphorylation status of BACE1 at Ser498 affects the rate at which BACE1 transits the early endosomes to the recycling endosomes and have identified a role for retromer and GGA1 in this transport process. Our findings show that there are multiple pathways from the early endosomes to the recycling endosomes and that specific sorting signals enhance the efficiency of the trafficking of membrane cargoes along this transport route.

temperature to 37°C for various times before fixation and permeabilization. Cells were stained for the internalized BACE1-antibody complexes with Alexa-conjugated secondary antibodies and antibodies to either (H) Rab11, (I) EEA1, or (J) CD63. The percentage of the BACE1 at early endosomes or recycling endosomes or late endosomes at each time point was calculated from the percentage of total BACE1 pixels that overlapped with EEA1, Rab11, or CD63, respectively. All calculations were performed using the OBCOL plug-in on ImageJ ($n = 15$ for each marker from three independent experiments). (K) HeLa cells stably expressing APP_{695wt} and endogenous BACE1 were transfected with either control siRNA or SNX4 siRNA for 72 h and conditioned media containing secreted APP processing products were analyzed for Aβ using a sandwich ELISA specific for $A\beta_{40}$. The levels of $A\beta_{40}$ for each sample were normalized against total cell protein levels using a Bradford assay. Data from four independent experiments. (L) Expression of an siRNA-resistant GFP-SNX4 construct (+Rescue) in SNX4 siRNA-treated HeLa cells. Seventy-two hours after transfection with siRNA monolayers were transfected for 24 h with wtBACE1 and the GFP-SNX4 construct as indicated, and monolayers permeabilized and stained for BACE1 (red) and CD63 (green). (M) The percentage of the BACE1 at late endosomes at each condition was calculated from the percentage of total BACE1 pixels that overlapped with CD63. All calculations were performed using the OBCOL plug-in on ImageJ. (D–M) Data are presented as mean ± SEM. $^{**}p < 0.01$, $^{***}p < 0.001$.

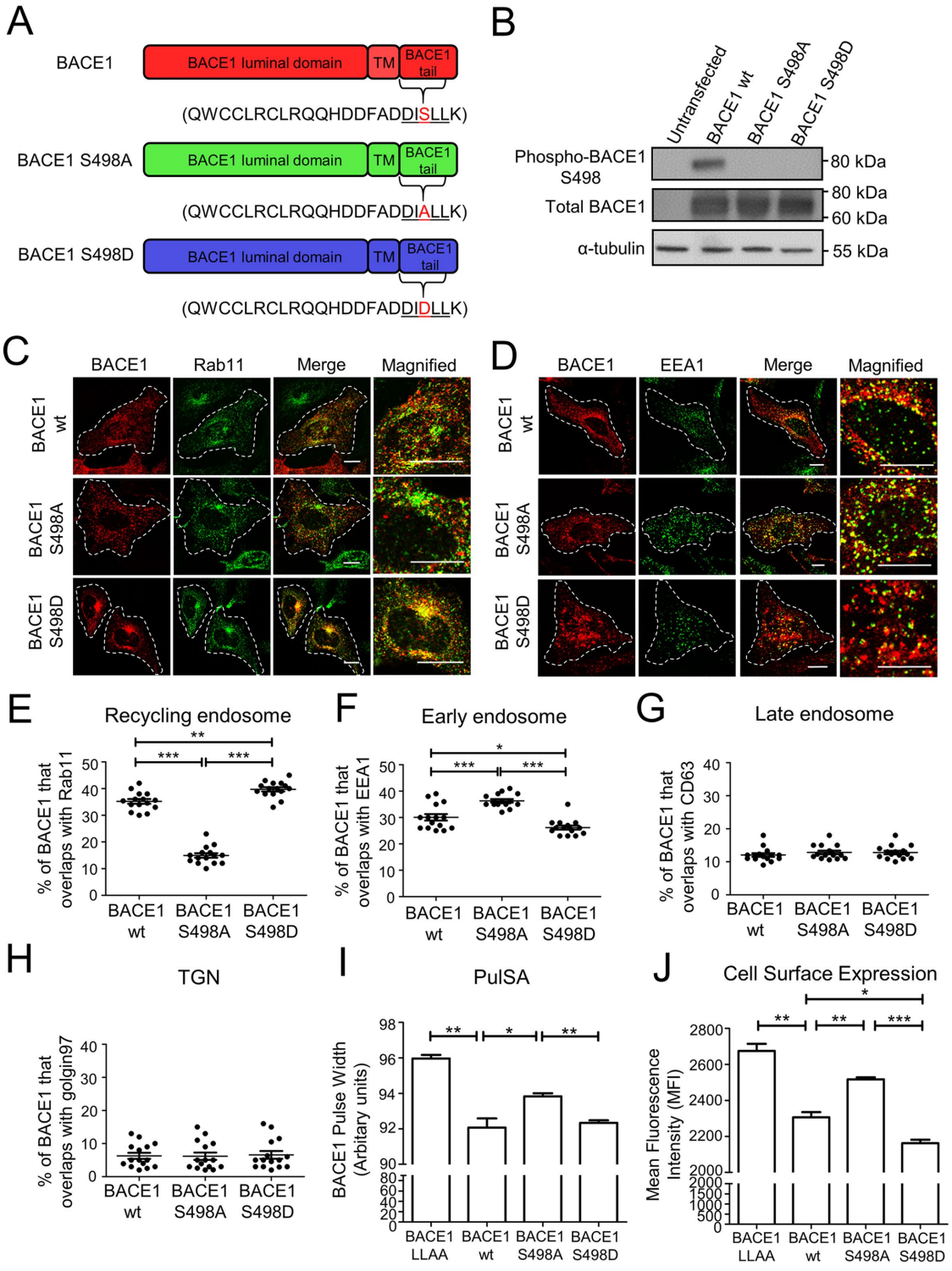

FIGURE 2: BACE1 phospho-mutants show differences in steady-state distribution and cell-surface expression in HeLa cells. (A) Schematic representation of BACE1 showing the luminal, transmembrane, and cytoplasmic domains. Ser498 in BACE1 was substituted with either an alanine or aspartate to mimic an unphosphorylated (green) or phosphorylated (blue) form of BACE1. (B) Immunoblotting of cell extracts of HeLa cells transfected with either wtBACE1 or BACE1 phosphomutants for 24 h and probed with rabbit anti-pSer498 BACE1 antibodies, rabbit anti-BACE1 antibodies, and mouse anti–α-tubulin antibodies, using a chemiluminescence detection system. (C, D) Confocal microscopic images of fixed and permeabilized HeLa cells transfected with either wtBACE1 or BACE1 phosphomutants and stained with rabbit polyclonal anti-human BACE1 antibodies (red) and mouse monoclonal antibodies to (C) Rab 11 or (D) EEA1 (green). Higher magnifications of the merge images are also shown. Bars represent 10 μm. (E–H) Percentage of BACE1 at the early endosomes, recycling endosomes, late endosomes, or the TGN was calculated from the percentage of total BACE1 pixels that overlapped with (E) Rab11, (F) EEA1, (G) CD63, or (H) golgin97, respectively. All calculations were

RESULTS

Depletion of SNX4 redirects BACE1 to the late endosomes

Previously, we demonstrated that BACE1 is internalized from the PM and transported to recycling endosomes via the early endosomes (Chia *et al.*, 2013), whereas APP is transported from the early endosomes to the late endosomes/lysosomes (Chia *et al.*, 2013; Toh *et al.*, 2016). The diversion of BACE1 from the endolysosomal pathway to the recycling endosomes represents an important transport step as it segregates BACE1 from APP and potentially limits APP processing. Here we have investigated the mechanisms that regulate endosomal sorting of BACE1. SNX4 has been identified as an essential component for sorting transferrin receptor to recycling endosomes (Traer *et al.*, 2007); therefore, we initially examined whether SNX4 also regulates BACE1 trafficking. Small interfering RNA (siRNA) treatment of HeLa cells reduced SNX4 protein levels by ~80% (Figure 1A). SNX4 depletion resulted in a reduction in colocalization of BACE1 with Rab11, a marker for recycling endosomes (Figure 1, B and D), and an increase in the colocalization of BACE1 with both the early endosome marker EEA1 (Figure 1E and Supplemental Figure S1C) and the late endosome marker, CD63 (Figure 1, C and F). Dotplots of the primary data are shown in Figure 1 (D–G) to demonstrate the low variance of each data set. There was also extensive colocalization of BACE1 and the transferrin receptor (TfR) under both control and SNX4-depleted conditions (Figure 1G and Supplemental Figure S1D), and, moreover, TfR also showed extensive colocalization with the late endosome marker Lamp1 in SNX4-depleted cells, as expected (Supplemental Figure S1E). A similar relocalization of BACE1 to late endosomes was observed with a second independent SNX4 siRNA (Supplemental Figure S1, A and B). To further exclude off-target effects of the siRNAs, SNX4 siRNA-treated cells were transfected with a GFP-SNX4 rescue construct; BACE1 showed a similar distribution in rescued cells as control cells (Figure 1, L and M), demonstrating that the perturbation in BACE1 distribution following RNAi was SNX4 specific. Therefore, these data indicate that BACE1 trafficking is regulated by SNX4. In addition, we assessed the effect of SNX4 depletion on the intracellular distribution of M6PR, a membrane receptor that recycles between early and late endosomes and the TGN. SNX4 depletion had no apparent effect on the distribution of M6PR and the colocalization with the TGN marker golgin97 (Supplemental Figure S2A), consistent with previous findings (Traer *et al.*, 2007) and demonstrating that SNX4 is required for the selective transport to the recycling endosomes and not the TGN. Silencing SNX4 also had no apparent effect on the level of colocalization of APP with the late endosome marker Rab7 (Supplemental Figure S2B), consistent with the transport of APP from the early endosomes along the endolysosomal pathway (Toh *et al.*, 2016).

To further investigate the influence of SNX4 on BACE1 sorting, we tracked the intracellular itinerary of BACE1 in control and SNX4-depleted cells using an antibody internalization assay. Transfected cells were incubated with anti-BACE1 antibodies for 30 min on ice, unbound antibodies were removed, and the temperature was shifted to 37°C to allow surface antibody-BACE1 complexes to internalize. The transport of BACE1 was tracked over a period of 90 min. SNX4 depletion had no apparent effect on endocytosis of BACE1 into early endosomes (Figure 1I, 15 min). However, compared with control siRNA-treated cells, SNX4-depleted cells had a reduced level of BACE1 that colocalized with Rab11 (Figure 1H and Supplemental Figure S3A) and an increased level of BACE1 that colocalized with CD63 (Figure 1J and Supplemental Figure S3B) after internalization for either 15 min or 90 min. By 90-min internalization, >20% BACE1 was detected in the late endosome compared with 4.8% in control treated cells. Taken together, these data show that SNX4 is essential for endosomal sorting of BACE1 from the endosomal/lysosomal pathway to the recycling endosome.

Depletion of SNX4 increased Aβ production

Given the finding that BACE1 was routed to the late endosomes in SNX4-depleted cells, we then assessed whether this altered trafficking of BACE1 influenced BACE1-mediated processing of APP and Aβ production. Here we used HeLa cells stably expressing APP_{695wt} (wild type [wt]) to assess levels of secreted Aβ, a cell line that also expresses endogenous BACE1. Conditioned media were collected from HeLa cells stably expressing APP_{695wt} and analyzed for the presence of Aβ using a sandwich enzyme-linked immunosorbent assay (ELISA) specific for $Aβ_{40}$; there was a 2.4-fold increase in secreted Aβ from SNX4-depleted cells compared with untreated cells (Figure 1K). Therefore, redirecting the transport of BACE1 from recycling endosomes to the late endosomes, following knock down of SNX4 increases Aβ production, findings that identify SNX4 as an important regulator of BACE1 trafficking and APP processing.

The immediate product of APP cleavage by BACE1 is membrane associated β-CTF (C99). Only very low levels of β-CTF were detected in either control or SNX4-depleted cells (data not shown), consistent with our previous observations that β-CTF is rapidly processed by γ-secretases to release Aβ (Toh *et al.*, 2016) and that BACE1 cleavage of APP is the rate-limiting step in the production of Aβ.

Impact of phosphorylation of the BACE1 DISLL motif on intracellular trafficking

SNX4 is considered to mediate a signal-independent transport pathway to the recycling endosomes (Traer *et al.*, 2007). However, we considered the possibility that sorting signals may also contribute a role to the endosomal sorting and transport of BACE1 to recycling endosomes, as phosphorylation of Ser498 within the DISLL motif of BACE1 has been reported to influence BACE1 intracellular trafficking (Walter *et al.*, 2001). To investigate a potential role of phosphorylation of Ser498 in endosomal sorting, Ser498 was mutated to either an alanine or aspartic acid to mimic a nonphosphorylated or phosphorylated form of BACE1, respectively (Figure 2A). The level of phosphorylation of wtBACE1 and the two mutants was

performed using the OBCOL plug-in on ImageJ ($n = 15$ for each marker from three independent experiments). (I) PulSA analyses. HeLa cells transfected with either wtBACE1 or BACE1 phosphomutants were harvested, fixed, and permeabilized; stained with rabbit polyclonal anti-human BACE1 antibodies; and analzyed by flow cytometry (FACS) for the pulse width of the fluorescent signal. Histograms show the mean pulse width and SEM from three independent experiments. (J) Cell-surface expression of HeLa cells transfected with either wtBACE1 or BACE1 phosphomutants. Viable cells in suspension were incubated with anti-BACE1 antibodies on ice for 30 min, fixed in 4% PFA, stained with Alexa488-conjugated IgG, and analyzed by FACS. Histograms shows the mean fluorescence intensity of cell-surface BACE1 normalized for the total BACE1 protein level for each BACE1 variant. Shown is the mean and SEM for three independent experiments. Bars represent 10 μm. (E–J) $*p < 0.05$, $**p < 0.01$ $***p < 0.001$.

analyzed by immunoblotting of extracts of transfected HeLa cells with an antibody specific for phosphorylated BACE1 at Ser498. Whereas wtBACE1 and the two BACE1 mutants S498A and S498D had similar levels of expression in transfected HeLa cells, only wtBACE1 showed a signal with antibodies to phosphoBACE1 S498 (Figure 2B) confirming the changes in phosphorylation status of the mutants.

The steady-state distribution of the BACE1 mutants was examined. Both wtBACE1 and BACE1 S498D localized strongly to the juxtanuclear region of the cell, the location of recycling endosomes, whereas BACE1 S498A showed less juxtanuclear staining. Moreover, BACE1 S498D showed increased levels of colocalization with Rab11 compared with wtBACE1 (Figure 2, C and E), while BACE1 S498A showed a reduction in the level of colocalization with Rab11 compared with wtBACE1 (Figure 2, C and E). Similar findings were observed for the neuroblastomona line SK-N-SH, namely wtBACE1 and BACE1 S498D showed an extensive overlap with Rab11 in transfected SK-N-SH cells while BACE1 S498A showed reduced overlap with Rab11 (Supplemental Figure S4A).

We then assessed the colocalization of the phosphomutants with early endosomes, late endosomes, and the TGN. BACE1 S498A, which has a more peripheral distribution in the cell, was found to colocalize with the early endosome marker EEA1 at a higher level compared with wtBACE1 and BACE1 S498D, whereas BACE1 S498D colocalized with EEA1 slightly less than wtBACE1 (Figure 2, D and F, and Supplemental Figure S4B). wtBACE1 and the phosphomutants all showed only low levels of colocalization the late endosome marker CD63 (Figure 2G) and with the TGN marker golgin97 (Figure 2H), indicating that the BACE1 phosphorylation did not redirect BACE1 to the TGN or the late endosomes. Overall, the data suggest that under steady-state conditions BACE1 S498A is localized more extensively in early endosomes while BACE1 S498D is localized more extensively to the recycling endosomes compared with wtBACE1.

Use of pulse-shape analysis (PulSA) to distinguish the distribution of BACE1 mutants in a large cell population

To further authenticate the intracellular distribution of the BACE1 variants within the cell population rather than a limited number of cells as analyzed by microscopy, we used a flow cytometry-based method that involves the measurement of the pulse width and height of a fluorescently labeled molecule simultaneously, called PulSA. Traditionally, data obtained from the pulse width has been used to discriminate single cells from clumped cells (Wersto *et al.*, 2001). However, PulSA can also be used for analysis of protein localization in a cell at high throughput (Ramdzan *et al.*, 2012; Chia *et al.*, 2014). We previously demonstrated that PulSA can distinguish among the location of membrane proteins at the PM, early endosomes, and Golgi (Chia *et al.*, 2014). PulSA can also be used to distinguish location of proteins at the PM, early endosomes, and recycling endosomes (Supplemental Figure S4C). To apply PulSA to analyze the BACE mutants, HeLa cells were transfected with wtBACE1, BACE1 phosphomutants, or with BACE1 LLAA, a BACE1 mutant that is endocytosis defective and is expected to be retained at the cell surface. Twenty-four hours after transfection, cells were harvested, fixed, permeabilized, and stained with BACE1 antibodies in suspension. Analyses of cell populations (10,000 cells) using PulSA showed a broader pulse width of fluorescently labeled BACE1 LLAA mutant compared with wtBACE1 (Figure 2I). BACE1 LLAA mutant showed the largest pulse-width measurement consistent with a defect in endocytosis and is localization predominantly at the cell surface (Prabhu *et al.*, 2012; Chia *et al.*, 2013). BACE1 S498A showed a higher pulse-width measurement compared with both wtBACE1 and BACE1 S498D (Figure 2I), indicating a more dispersed and peripheral location of S498A compared with either wtBACE1 or BACE1 S498D. These PulSA analyses confirm an altered intracellular distribution of the phosphoBACE mutants and are consistent with the predominant location of BACE1 S498D in the perinuclear recycling endosomes, whereas the S498A mutant is more concentrated in the peripheral early endosomes.

Cell-surface expression of BACE1 phosphomutants is altered

Given the alterations in the intracellular distribution of the phosphoBACE1 mutants the question arises whether there are also changes in the recycling efficiency of BACE1 to the PM. Therefore, we analyzed levels of surface expression of the BACE1 constructs in transfected HeLa cell by flow cytometry of surface-labeled nonpermeabilized cells. Cell-surface expression of each construct was normalized to the total cellular BACE1 level for each BACE1 construct. As expected, BACE1 LLAA showed the highest levels of cell-surface expression (Figure 2J). Interestingly, BACE1 S498A showed a significant increase in cell-surface expression compared with wtBACE1, while BACE1 S498D showed a reduction in cell-surface expression compared with wtBACE1 (Figure 2J). These findings suggest that the two BACE1 mutants differ in their capacity to be transported back to the PM from endosomal compartments.

Intracellular itinerary of phosphoBACE1 mutants in HeLa cells

To further investigate the differences in distribution of the BACE1 phosphomutants, we tracked the movement of the BACE1 mutants from the PM to the early endosomes and recycling endosomes. HeLa cells were transfected with either wtBACE1 or the phosphomutants for 24 h and then incubated with anti-BACE1 antibodies for 30 min on ice, unbound antibodies were removed, and the temperature was shifted to 37°C to allow surface antibody-BACE1 complexes to internalize. The transport of BACE1 constructs was tracked over a period of 90 min. As expected, at 0 min wtBACE1 and the phosphomutants were localized to the cell surface (not shown). After 15 min at 37°C, all BACE1 variants were efficiently internalized, and a similar percentage (~40%) of the antibody-BACE1 complexes for each construct was detected in early endosomes (Figure 3A). Extended periods at 60 min and 90 min at 37°C showed a subsequent reduction in the percentage of BACE1 constructs located in early endosomes; however, there were significant differences in the levels of each construct after 60 or 90 min. BACE1 S498A showed an increased colocalization with EEA1 compared with wtBACE1 after 60- and 90-min internalization, while there was a significantly reduced level of BACE1 S498D in the early endosomes compared with wtBACE1 (Figure 3A). All three constructs were detected in Rab11-positive recycling endosomes after 15 min at 37°C, and these levels increased over the 90-min period (Figure 3B). Notably, there was an increased level of BACE1 S498D in the recycling endosomes compared with wtBACE1 or BACE1 S498A by 15-min internalization that continued to increase over the 90-min period. These results suggest that BACE1 S498D is transported out of the early endosomes at a faster rate than both wtBACE1 and BACE1 S498A. In contrast, BACE1 S498A appears to be transported more slowly from the early endosomes to the recycling endosomes compared with wtBACE1 or BACE1 S498D.

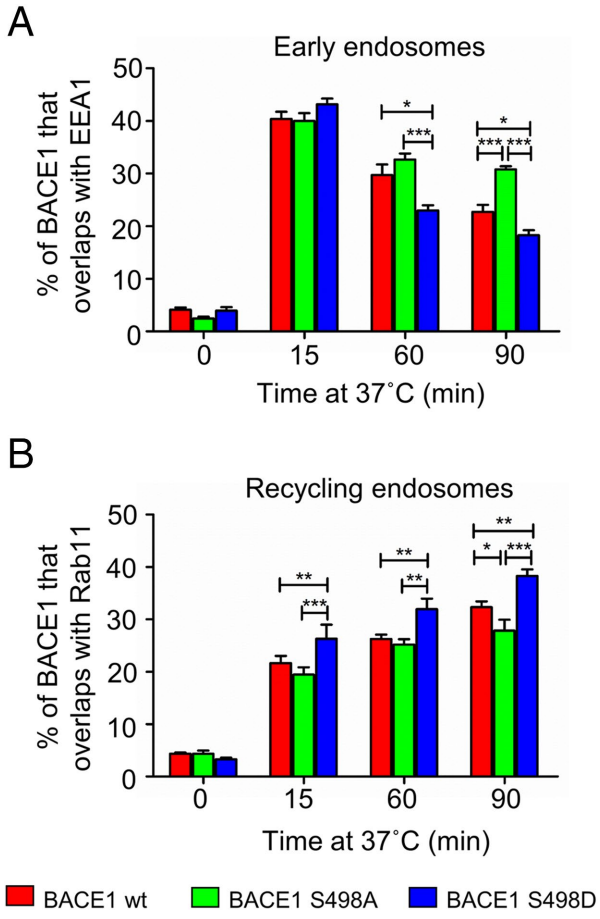

FIGURE 3: BACE1 phosphomutants in HeLa cells exhibit different rates of transport from the early endosomes. (A, B) HeLa were transfected with either wtBACE1 or BACE1 phosphomutants for 24 h. Transfected cells were incubated with anti-BACE1 antibodies on ice for 30 min, washed in cold PBS, and, for the 0-min time point, immediately fixed and permeabilized. For internalization of the antibody-BACE1 complexes, monolayers were shifted to 37°C for various times before fixation and permeabilization. Cells were then stained for BACE1–antibody complexes with Alexa-conjugated secondary antibodies and either (A) EEA1 or (B) Rab11 using monoclonal antibodies to EEA1 and mouse monoclonal antibodies to Rab11, respectively. The percentage of the BACE1 phosphomutants at the early endosomes or recycling endosomes at each time point was calculated from the percentage of total BACE1 pixels that overlapped with EEA1 or Rab11, respectively. All calculations were performed using the OBCOL plug-in on ImageJ. Data were pooled from three independent experiments and are expressed as the mean ± SEM ($n = 15$) and analyzed by an unpaired, two-tailed Student's t test. *$p < 0.05$, **$p < 0.01$, ***$p < 0.001$.

Retromer and GGA1 are required for the enhanced trafficking of BACE1 S498D to the recycling endosomes

Given the finding that pSer498 promotes rapid transport of BACE1 to the recycling endosomes, we then investigated the role of retromer in mediating this signal-dependent transport process. The retromer subunit Vps26 was silenced in HeLa cells with previously characterized human Vps26 siRNA target sequences (Popoff *et al.*, 2007). Immunofluorescence and immunoblotting showed that the protein level of Vps26 was significantly reduced (~85%) in Vps26 siRNA-transfected cells (Figure 4, A and B). Knock down of Vps26 resulted in an alteration in the steady-state distribution of wtBACE1 and S498D BACE1 mutant with an increase in levels that colocalized with the early endosome marker EEA1 (Figure 4C) and a concomitant and dramatic reduction in levels that colocalized with Rab11 (Figure 4D and Supplemental Figure S5A). Expression of a Vps26A siRNA-resistant construct in Vps26 siRNA-treated cells restored levels of both wtBACE1 and S489D mutant that colocalized with Rab11 (Figure 4E), demonstrating a Vps26-specific rescue of the altered location. On the other hand, there was no significant change in the distribution of the BACE1 S498A mutant between early endosomes and recycling endosomes in Vps26-depleted cells (Figure 4, C and D), indicating that the pSer498-mediated trafficking was retromer dependent. Silencing the retromer subunit Vps35 also showed a similar effect with increased levels of wtBACE1 that colocalized with the early endosome marker EEA1 (Supplemental Figure S6), confirming the role of retromer in this process.

GGA1 has been shown to bind to BACE1, and this binding has been shown to be enhanced by Ser498 phosphorylation (Shiba *et al.*, 2004). Therefore, we also investigated whether GGA1 may be relevant for endosomal sorting and transport of the phosphoBACE1 to the recycling endosomes. Using a previously defined siRNA target sequence for GGA1, we obtained effective reduction (~75%) of GGA1 levels, as assessed by immunofluorescence and immunoblotting (Figure 5, A and B). Analysis of steady-state distribution of BACE1 and phosphoBACE1 mutants following knock down of GGA1 revealed increased levels in wtBACE1 and S498D mutant that colocalized with the early endosome marker EEA1 (Figure 5C and Supplemental Figure S6, C and D) and dramatic reduction that colocalized with the recycling endosome marker Rab11 (Figure 5D and for confocal images Supplemental Figure S5A). Expression of a siRNA GGA1-resistant construct in GGA1 siRNA-treated cells rescued the altered location of the wtBACE1 and S498D mutant, ruling out off-target effects of the GGA1 siRNA (Figure 5E). In contrast, the distribution of the BACE1 S498A mutant was unchanged between early and recycling endosomes in GGA1 knock-down cells, results very similar to the findings in Vps26-depleted cells (Figure 5, C and D). On the other hand, the distribution of the TfR remained concentrated in the perinuclear region following knock down of GGA1 (Supplemental Figure S5B).

We also tracked the movement of the BACE1 mutants from the PM to the early endosomes and recycling endosomes in GGA1-depleted cells. HeLa cells were transfected with GGA1 siRNA and then subsequently with either wtBACE1 or the phosphomutants for 24 h, and an internalization assay was performed as in experiments above. The kinetics of intracellular trafficking of wtBACE1, S498D, and S498A mutants in control siRNA-treated cells (Figure 6) was very similar to the previous experiment in Figure 3 with the S498D mutant accumulating in recycling endosomes more rapidly than wtBACE1 (Figure 6C); however, in GGA1 siRNA-treated cells there was no difference in the distribution between the two phosphomutants and wtBACE1 constructs (Figure 6, A–C). wtBACE1 and S498D and S498A mutants were all transported to recycling endosomes at a similar rate (Figure 6, A and C); and the kinetics of transport corresponded to the rate of the nonphosphomimetic S498A in control siRNA-treated cells. Likewise, in GGA1-depleted cells, wtBACE1 and the two phosphomutants all showed similar levels in the early endosomes over a 60-min period of internalization (Figure 6, A and B), rates that were also similar to the S498A mutant in control siRNA-treated cells. Hence the silencing of GGA1 abrogates the enhanced trafficking of the phosphomimetic S498D mutant from the early endosome to the recycling endosomes.

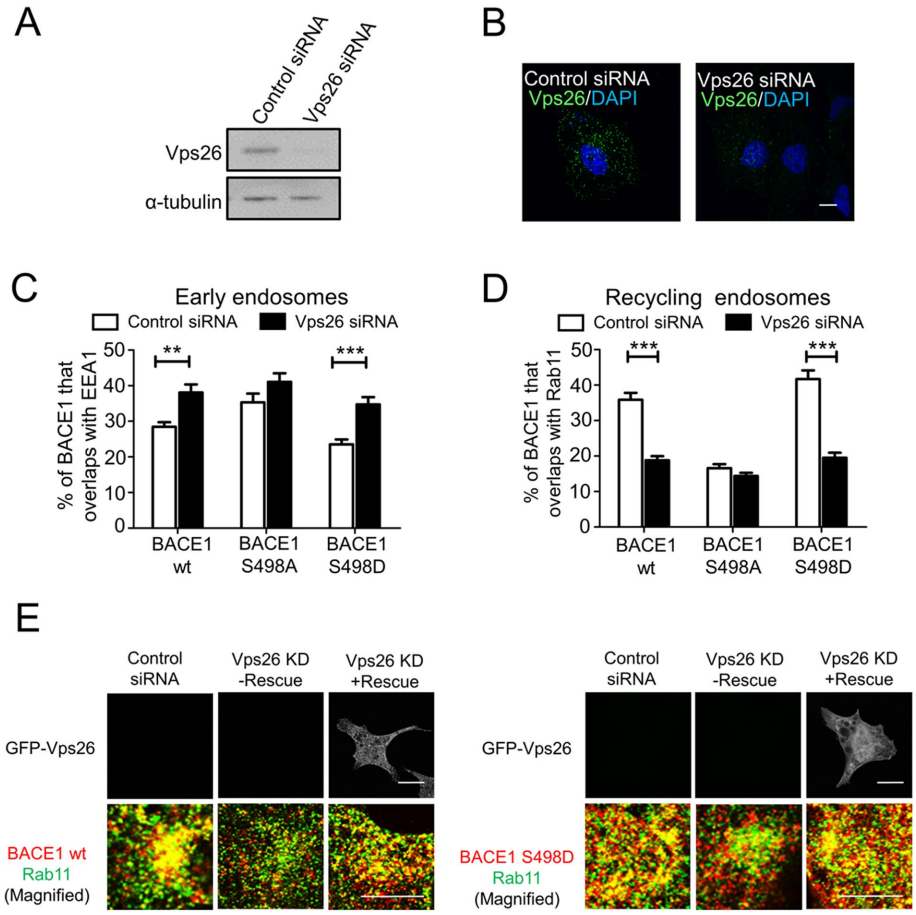

FIGURE 4: Vps26 regulates the steady-state distribution of BACE1 phosphomutants. (A) Immunoblotting of cell extracts of HeLa cells transfected with either control siRNA or Vps26 siRNA for 72 h and probed with rabbit anti-Vps26 and mouse anti–α-tubulin antibodies, using a chemiluminescence detection system. (B) Confocal microscopic images of fixed and permeabilized HeLa cells transfected with either control siRNA or Vps26 siRNA for 72 h and stained with rabbit polyclonal anti-Vps26 antibodies and DAPI. Bars represent 10 μm. (C, D) Percentage of wt BACE1 and BACE1 phosphomutants in HeLa cells transfected with either control siRNA or Vps26 siRNA at the early endosomes (C) and recycling endosomes (D) was calculated from the percentage of total BACE1 pixels that overlapped with EEA1 and Rab11. Monolayers were stained with rabbit polyclonal anti-human BACE1 antibodies and (C) mouse monoclonal antibodies to EEA1 or (D) mouse monoclonal antibodies to Rab11. In C and D, calculations were performed using the OBCOL plug-in on ImageJ. Data were pooled from three independent experiments and are expressed as the mean ± SEM ($n = 15$) and analyzed by an unpaired, two-tailed Student's t test. $^{**}p < 0.01$, $^{***}p < 0.001$. (E) Expression of an siRNA-resistant GFP-Vps26A construct (rescue) in Vps26 siRNA-treated cells. Monolayers were stained with rabbit polyclonal anti-human BACE1 antibodies (red) and mouse monoclonal antibodies to Rab11 (green). Bar represents 10 μm.

Signal-dependent GGA1 pathway is independent of the SNX4 pathway

The question arises whether GGA1-mediated sorting of BACE1 represents an independent transport pathway from the SNX4-mediated pathway or whether the two processes are coordinated within the same pathway. We addressed this question by two independent approaches. First, we performed a simultaneous knock down of both SNX4 and GGA1 and analyzed the impact on the intracellular distribution of wtBACE1. Depletion of both SNX4 and GGA1 resulted in a dramatic reduction of BACE1 at the recycling endosomes and a dramatic increase in the level of BACE1 at the late endosomes (Figure 7, A and B). Significantly, there was an additive effect on reduction of BACE1 at the recycling endosomes, and an increase of BACE1 at the late endosomes (Figure 7, B–E), compared with SNX4 single knock downs (Figure 1, D and F). This result indicates that the two transport processes do not share the same pathway.

Second, we assessed the impact of silencing SNX4 on the distribution of the two BACE1 phosphomimetic mutants, S498A and S498D. SNX4 knock down of S498A showed a reduction of this BACE1 mutant at the recycling endosomes to <10% (Figure 7, F and G), demonstrating that the nonphosphomimetic S498A mutant was using the SNX4 pathway to be transported to the recycling endosomes. On the other hand, SNX4 knock down had minimum effect on the distribution of the phosphomimetic S498D mutant. The levels of BACE1 S489D in the recycling endosomes of SNX4-depleted cells (40%) was similar to control siRNA-treated cells (Figure 7, H and I), and, moreover, only low levels of BACE1 S489D were detected in CD63-positive late endosomes (not shown). Thus, S498D can be transported by the GGA1 pathway in the absence of SNX4. Hence, these two distinct approaches support the presence of two independent pathways from the early endosomes to the recycling endosomes, a signal-mediated GGA1-dependent pathway, and a signal-independent SNX4 pathway.

Aβ production is altered by BACE1 mutants

To determine whether the BACE1 variants would modulate Aβ generation, CHO cells stably expressing both APP and wtBACE1 or the phosphomutants were generated. CHO cells were used in these experiments as we had previously defined the processing of APP in stable CHO cells (Chia *et al.*, 2013). The expression of wtBACE1 or the BACE1 phosphomutants in the CHO cell lines were assessed by immunoblotting (Figure 8A) and the expression levels of each BACE1 variant found to be very similar (Figure 8A). Conditioned media containing secreted APP processing products were analyzed for the presence of Aβ using a sandwich ELISA specific for $Aβ_{40}$. The levels of Aβ for each sample were normalized against total cell protein levels using a Bradford assay (not shown) and then normalized against total BACE1 levels for each BACE1 variant. The $CHO_{BACE1\ S498A}$ stable cell line produced threefold more Aβ than the $CHO_{BACE1wt}$ stable cell line while the $CHO_{BACE1\ S498D}$ cells produced 30% less Aβ than the $CHO_{BACE1wt}$ stable cells (Figure 8B). Taken together, these results suggest that the changes in the intracellular distribution of BACE1 have a profound effect on Aβ generation.

Distribution of BACE1 mutants is altered in primary neurons

We also assessed the relevance of our findings in primary neurons as amyloid deposits in AD is due to Aβ production and secretion by

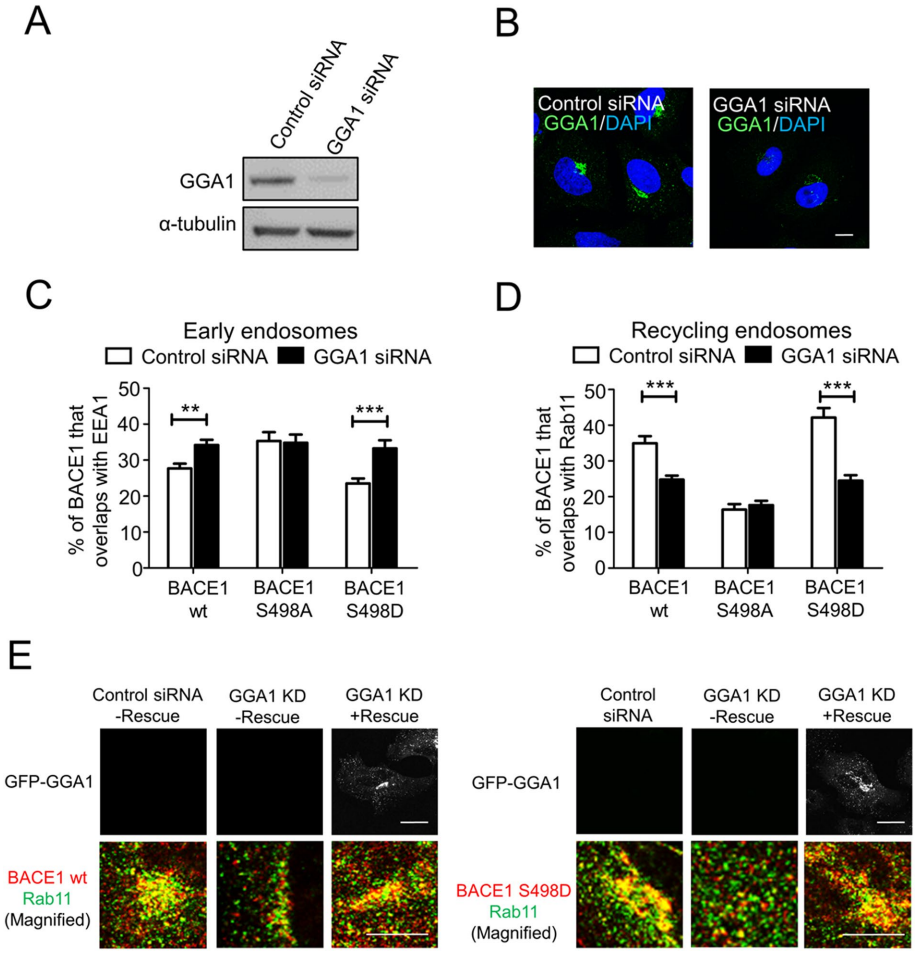

FIGURE 5: GGA1 regulates the steady-state distribution of BACE1 phosphomutants. (A, E) Immunoblotting of cell extracts of HeLa cells transfected with either control siRNA or GGA1 siRNA for 72 h and probed with rabbit anti-GGA1 antibodies and mouse anti–α-tubulin antibodies, using a chemiluminescence detection system. (B) Confocal microscopic images of fixed and permeabilized HeLa cells transfected with either control siRNA or GGA1 siRNA for 72 h and stained with rabbit monoclonal anti-GGA1 antibodies and DAPI. Bars represent 10 μm. (C, D) Percentage of wtBACE1 and BACE1 phospho-mutants in HeLa cells transfected with either control siRNA or GGA1 siRNA at the (C) early endosomes and (D) recycling endosomes was calculated from the percentage of total BACE1 pixels that overlapped with EEA1 and Rab11. Monolayers were stained with rabbit polyclonal anti-human BACE1 antibodies and (C) mouse monoclonal antibodies to EEA1 or (D) mouse monoclonal antibodies to Rab11. In C and D, calculations were performed using the OBCOL plug-in on ImageJ. Data were pooled from three independent experiments and are expressed as the mean ± SEM ($n = 15$) and analyzed by an unpaired, two-tailed Student's t test. $^{**}p < 0.01$, $^{***}p < 0.001$. (E) Expression of an siRNA-resistant GFP–GGA1 construct (rescue) in GGA1 siRNA-treated cells. Monolayers were stained with rabbit polyclonal anti-human BACE1 antibodies (red) and mouse monoclonal antibodies to Rab11 (green). Bar represents 10 μm.

neurons. Cortical primary neurons were cultured from E16 mouse embryos for 7 d and then transiently transfected with the BACE1 constructs for 24 h, fixed, and stained with BACE1 antibodies. The BACE1 antibodies used in this experiment detect only the exogenous BACE1 and do not detect endogenous BACE1 in untransfected neurons (Figure 9A). In primary neurons, transfected wtBACE1 showed colocalization with both the recycling endosome marker Rab11 and the early endosome marker Rab4 (Figure 9, B and C). The BACE1 S498A mutant showed a higher level of colocalization with Rab4 than Rab11, whereas BACE1 S498D colocalized more extensively with Rab11 than Rab4 (Figure 9, B and C). Thus, the phosphomutants have distinct intracellular distributions in primary neurons, distributions similar to both HeLa and SK-N-SH cells.

We also assessed the phosphorylation status of DISLL motif in endogenous BACE1 from primary neuron cultures. Blotting of extracts of unstimulated neurons with an antibody specific for pSer498 BACE1 detected a 78-kDa component. Treatment of the cell extracts with phosphatase eliminated the reactivity with the anti-pSer498 antibody, confirming the identity of the 78-kDa component as pSer498 BACE1. Neuronal stimulation and excitotoxicity via the *N*-methyl-D-aspartate (NMDA) glutamate receptor is thought to contribute to a number of neurodegenerative diseases (Danysz and Parsons, 2012). Here we analyzed the phosphorylation of BACE1 following stimulation with NMDA. We detected a 2.3-fold increase in the levels of pSer498 BACE1 following NMDA stimulation, indicating that the posttranslational modification of DISLL is modified by signaling events (Figure 9, D and E). These findings strongly indicate that the phosphorylation of DISLL influences endosomal trafficking of BACE1 in neurons and, moreover, the level of phosphorylation of the DISLL motif can be regulated by signaling.

DISCUSSION

The intracellular trafficking of BACE1 is central to the regulation of APP processing; the initial cleavage of APP by BACE1 is the rate-limiting step in the generation of Aβ and a target for therapeutic intervention. Previous studies have shown that BACE1 is internalized from the PM to the early endosomes and then transported to the recycling endosomes for recycling to the PM; in contrast, newly synthesized APP is directly transported from the TGN to the early endosomes and then along the endolysosomal pathway (Burgos *et al.*, 2010; Toh *et al.*, 2016). Hence the early endosomes are an important convergence site for APP and BACE1. Dysfunctional endosomal trafficking of either BACE1 or APP has attracted considerable attention as an underlying defect associated with enhanced Aβ generation. Several AD susceptibility genes are associated with the regulation of membrane trafficking (Scherzer *et al.*, 2004; Andersen *et al.*, 2005; Small *et al.*, 2005; Rogaeva *et al.*, 2007; Muhammad *et al.*, 2008; Ginsberg *et al.*, 2011; Vardarajan *et al.*, 2012), and there is evidence that defective membrane trafficking contributes to AD from animal models (Siegenthaler and Rajendran, 2012; Berman *et al.*, 2015; Small and Petsko, 2015). As BACE1 is segregated from APP at the early endosomes and transported to the recycling endosomes, the underlying molecular processes for endosomal sorting of BACE1 and transport to the recycling endosomes is important to define.

Here we have examined the endosomal sorting of BACE1 and demonstrated that there are two distinct processes for transport of

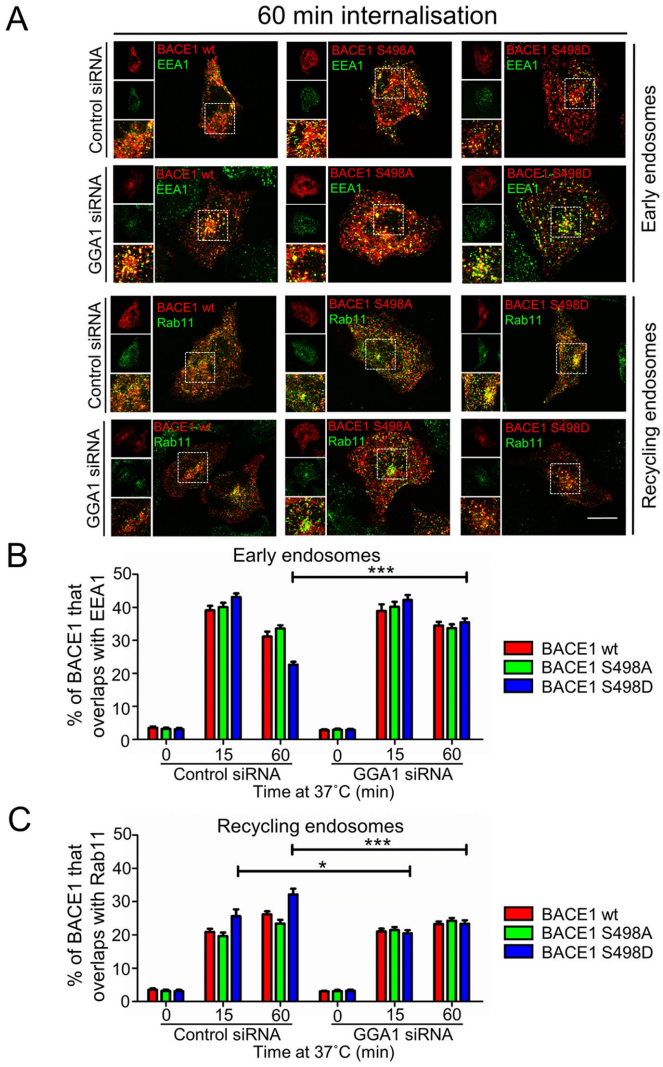

FIGURE 6: GGA1 depletion reduces trafficking of BACE1 S498D mutant from the early endosome to the recycling endosome. (A–C) HeLa cells were transfected with either control siRNA or GGA1 siRNA for 72 h and transfected with either wtBACE1 or BACE1 phosphomutants constructs for a further 24 h. Transfected cells were incubated with anti-BACE1 antibodies on ice for 30 min. For the 0-min time point, cells were washed in cold PBS and immediately fixed and permeabilized. Antibody-BACE1 complexes were internalized by shifting the temperature to 37°C for indicated times before fixation and permeabilization. Cells were stained for the internalized BACE1-antibody complexes with Alexa-conjugated secondary antibodies (red) and either EEA1 or Rab11 using mouse monoclonal antibodies to EEA1 or mouse monoclonal antibodies to Rab11 (green). (A) Confocal microscopic images after 60 min at 37°C. Bar represents 10 µm. (B, C) The percentage of wtBACE1 and the BACE1 phosphomutants at the early endosomes and recycling endosomes at each time point was calculated from the percentage of total BACE1 pixels that overlapped with (B) EEA1 or (C) Rab11, respectively. All calculations were performed using the OBCOL plug-in on ImageJ ($n = 15$ for each marker and timepoint from three independent experiments). Error bars represent SEM. *$p < 0.05$, ***$p < 0.001$,

BACE1 from the early endosomes to the recycling endosomes: 1) A SNX4-mediated pathway and 2) a sorting signal-mediated pathway dependent on the phosphorylation status of the DISLL motif of BACE1. The phosphomimetic, DIDLL, is transported at a faster rate to the recycling endosomes than either wtBACE1 or the nonphosphomimetic DIALL, results consistent with the reduced of levels S498D BACE1 in early endosomes under steady-state conditions. Perturbation of the signal-sorting pathway by either mutation of the Ser in the DISLL motif or by silencing GGA1 or retromer results in a ~30% reduction in the transport rate of BACE1 to the recycling endosomes. The pSer-DISLL-mediated trafficking of BACE1 is biologically relevant as elimination of the signal-sorting pathway resulted in a threefold increase in production of Aβ. Our findings strongly indicate that the phosphorylation of DISLL influences endosomal trafficking of BACE1 in both HeLa cells and primary neurons, and, moreover, the capacity to modulate the level of phosphorylation of the DISLL motif provides a dynamic mechanism for regulating the exit of BACE1 from an endosomal compartment shared with APP.

BACE1 shares a similar intracellular itinerary as TfR. Rab11 has previously been shown to be important for the transport of BACE1 from recycling endosomes to the PM (Udayar *et al.*, 2013); however, the machinery for transport to the recycling endosomes had not been defined. We initially investigated the role of SNX4 as SNX4 had been shown to regulate TfR trafficking (Ullrich *et al.*, 1996; Ren *et al.*, 1998; Traer *et al.*, 2007). SNX4 is associated with tubular elements of the early endosomes and shown to promote long-range transport to recycling endosomes by interactions with motor proteins (Traer *et al.*, 2007). There is no evidence that SNX4 interacts directly with cargo, and it has been proposed that SNX4 drives signal-independent geometric sorting of membrane cargo to the recycling endosomes (Traer *et al.*, 2007). When this default pathway to the recycling endosomes is blocked, additional membrane of the early endosomes will then be passaged along the late endosomal-lysosomal route. Our data showed that depletion of SNX4 reduced BACE1 localization in the recycling endosomes and increased localization of BACE1 in the early endosomes and late endosomes, similarly to the findings for TfR following SNX4 knock down (Traer *et al.*, 2007). As a consequence of SNX4 knock down, BACE1 will be co-transported with APP along the late endosome/lysoosmal route, thereby extending the length of time both APP and BACE1 are co-located in an acidic environment and enhancing APP processing. Although it is possible that the trafficking of APP may also be altered as a consequence of SNX4 knock down, we think this is unlikely as the levels of APP in the late endosomes did not appear to be affected by SNX4 depletion, and, in addition, we have previously demonstrated that APP traffics from the early endosome to the late endosome/lysosomal pathway (Chia *et al.*, 2013; Toh *et al.*, 2016) and is not diverted from endosomes to either the TGN or recycling endosomes. Our findings reveal that SNX4 is an important factor in regulating BACE1 trafficking and dysregulation in SNX4 function may increase Aβ production. Notably SNX4 has recently been identified as an AD susceptibility gene (Kim *et al.*, 2017).

BACE1 has been shown to be phosphorylated at Ser498 by casein kinase I or a casein kinase I-like kinase in vivo (Walter *et al.*, 2001). The phosphorylation of the DISLL sorting motif in the cytoplasmic tail of BACE1 has been shown to enhance BACE1 transport from the early endosomes (Walter *et al.*, 2001; Pastorino *et al.*, 2002; He *et al.*, 2005); however, the role of Ser498 phosphorylation in the transport of BACE1 to the recycling endosomes had not been investigated. Here we showed that the BACE1 S498A mutant is enriched in the early endosomes while the BACE1 S498D mutant is predominantly located to the recycling endosomes in both cultured cells and primary neurons. Neither wtBACE1 nor the phosphomutants accumulated in the TGN nor the late endosomes. The earlier studies analyzing BACE1 S498 mutants assessed their location in the TGN but not the recycling

endosomes (Walter *et al.*, 2001; Pastorino *et al.*, 2002; He *et al.*, 2005), and as both these compartments are in the perinuclear region of the cell, they can be difficult to discriminate. Our data clearly show a difference in distribution between the BACE1 constructs that is likely to be due to differences in kinetics of transport from the early endosomes. BACE1 S498D was shown to exit the early endosomes and traffic to the recycling endosomes at a faster rate compared with wtBACE1 and BACE1 S498A; therefore, the nonphosphorylated BACE1 S498A mutant has an extended residency time in the early endosomes. Our findings also show that alterations in distribution and kinetics of BACE1 transport impacts Aβ production. Indeed, there was a threefold increase in Aβ production by the BACE1 S498A mutant. The relationship between distribution of BACE mutants and the production of Aβ strongly supports the proposal that the recycling endosomes acts as a compartment to sequester BACE1 from APP and is protective against excessive Aβ production (Chia *et al.*, 2013).

The transport of BACE1 S498D mutant required both retromer and GGA1. GGAs have been reported to function at the TGN and also in the endolysosomal pathway (Bonifacino, 2004; Puertollano and Bonifacino, 2004; He *et al.*, 2005; Wahle *et al.*, 2005; Herskowitz *et al.*, 2012), and our work extends further the role of GGAs in endosomal sorting. Previous studies have suggested that members of the GGA family influence transport of BACE1 from the early endosomes (Tesco *et al.*, 2007; Kang *et al.*, 2010), and FRET analysis has demonstrated an interaction between GGA1 and BACE1 that is dependent on phosphorylation of the DISLL motif (von Arnim *et al.*, 2004). Our studies have demonstrated a direct role for GGA1 in transport of BACE1 to the recycling endosomes. Following GGA1 depletion, the transport of the S498D mutant from the early endosomes was identical to the S498A mutant. Retromer is also required for the transport of phosphorylated BACE1. GGA1 and retromer are colocalized at the early endosome (unpublished data), which is consistent with the respective roles of both adaptor and coat in this pathway. Retromer contributes to a number of endosomal pathways and has not generally been considered to be involved in the pathway(s) to the recycling endosomes, and hence this represents a novel finding. Retromer core subunits, for example, Vps26/29/35, can assemble with different sets of SNX components (Cullen and Korswagen, 2012) and it will be of interest to define the retromer variant that is relevant for the pathway to the recycling endosomes. Additional components are likely to also be important in regulating this GGA1 pathway. Notably sortilin, a Vps10p sorting receptor, has been shown to be important for the trafficking of BACE1 from early endosomes (Finan *et al.*, 2011) and may also be important in regulating the pathway we have identified in this study.

The level of BACE1 S498A was elevated at the PM compared with wtBACE1 and the S498D mutant, a finding which appears to be in contradiction to the reduced transport rate of the S498A mutant to the recycling endosomes. However, fast recycling of cargo directly between the early endosomes and the PM may explain increased levels of BACE1 S498A at the PM and in early endosomes compared with S498D. This scenario is also consistent with the increased APP processing by BACE1 S498A compared with wtBACE1 and BACE1 S498D.

Neuronal stimulation has been associated with increased levels of Aβ (Kamenetz *et al.*, 2003; Cirrito *et al.*, 2005; Bero *et al.*, 2011; Das *et al.*, 2013). Our finding that the BACE1 DISLL motif is phosphorylated in primary neurons and the phosphorylation levels increase following activation of glutamate receptors highlights the potential of signaling events to modulate trafficking of membrane cargo. Hence, DISLL phosphorylation links signaling, endosomal trafficking of BACE1, and the production of Aβ. As APP trafficking can also be modulated by phosphorylation on its cytoplasmic tail (Oishi *et al.*, 1997; Vieira *et al.*, 2009, 2010), the impact of intracellular trafficking of both BACE1 and APP following neuronal activation needs to be further examined.

On the basis of our findings, we suggest that BACE1 is trafficked to the recycling endosomes by two distinct mechanisms, as illustrated in Figure 10, which together provide the capacity to finely regulate endosomal sorting efficiency and residency time of BACE1 in the early endosome. First, a SNX4-dependent pathway, shared with the TfR, that does not rely on specific sorting signals and can transport either nonphosphorylated or phosphorylated BACE1 with equal efficiency. This pathway would involve partitioning of BACE1 into transport tubules promoted by the physical properties of SNX4 and involve bulk flow of membrane from the early endosomes to the recycling endosomes. Second, a GGA1- and retromer-mediated pathway where the adaptor GGA1 recognizes the phosphorylated DISLL motif of BACE1 and retromer drives tubulation and formation of transport carriers to promote rapid cargo transport to the recycling endosomes (see Figure 10). We propose that the signal-dependent GGA1-mediated pathway is independent from the SNX4 pathway based on our findings that knock down of GGA1 and SNX4 resulted in an additive effect on the transport of BACE1 and that the trafficking of the phosphomimetic BACE1 S498D mutant to recycling endosomes was unaffected by the absence of SNX4. We propose that the posttranslational modification of DISLL would allow the capacity to finely regulate the kinetics of transport along this pathway. Changes in the levels of phosphorylation of BACE1 would influence the transport kinetics of BACE1 from the early endosomes and the extent of processing of APP. How retromer and GGA1 act to promote cargo selection and formation of transport carriers is not clear at this stage. Other factors could be involved such as EH domain–containing protein (EHD), which has been implicated in transport to the recycling endosomes (McKenzie *et al.*, 2012). In addition, sortilin, a Vps10p sorting receceptor, has been shown to be important for the trafficking of BACE1 from early endosomes (Finan *et al.*, 2011) and may also be important in regulating the pathway we have identified in this study.

In summary, our findings have identified a pathway to the recycling endosomes involving specific sorting signals and distinct from the transferrin receptor. It will be of interest to determine whether other membrane cargoes, particularly those with acidic dileucine motifs, are also transported via the GGA1-mediated pathway. More generally, the capacity to modulate an endosomal sorting signal by phosphorylation provides a unique mechanism for regulated transport between two endosomal compartments.

MATERIALS AND METHODS

Plasmids and antibodies

pcDNA4/TO BACE1 vector was kindly provided by Michael Cater, Mental Health Research Institute, Victoria, Australia. Rabbit polyclonal antibodies to SNX1 have been described (Lim *et al.*, 2012). Rabbit polyclonal to β-secretase (BACE1) (N terminus 46–62, EE17) was obtained from Sigma Aldrich (Castle Hill, NSW, Australia). Mouse antibodies to golgin97 (A-21270) were from Life Technologies (Grand Island, NY). Mouse monoclonal antibodies to EEA1 (610456) and Rab11 (610656) were purchased from Transduction laboratories (BD Biosciences, North Ryde, NSW, Australia). When using mouse monoclonal Rab11 antibodies, antibodies were diluted in Can Get Signal Immunoreaction Enhancer Solution A (Toyobo Life Science Department, Japan). Mouse monoclonal antibodies to CD63 (SC-5275) and goat polyclonal antibodies to SNX4 (sc-10623) were obtained from Santa Cruz Biotechnology (Dallas, TX). Rabbit

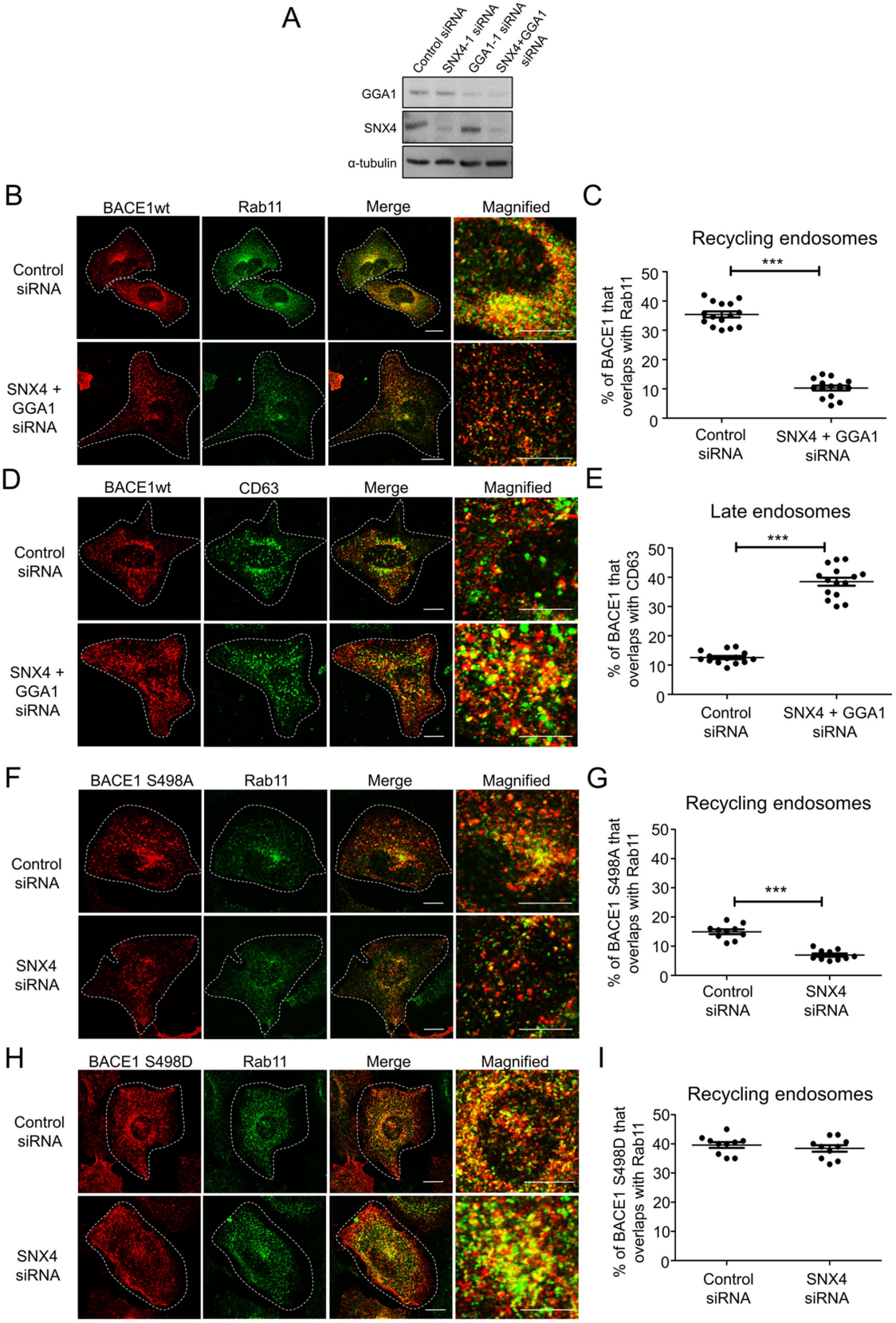

FIGURE 7: Trafficking of BACE1 mutants mediated by GGA1 to recycling endosomes is independent of the SNX4 transport pathway. (A–E) HeLa cells were transfected with either control siRNA or SNX4 and GGA1 siRNA for 72 h and transfected with the wtBACE1 construct for a further 24 h. (A) Immunoblotting of cell extracts with goat anti-SNX4 antibody, rabbit anti-GGA1 antibody and mouse anti–α-tubulin antibody, using a chemiluminescence detection

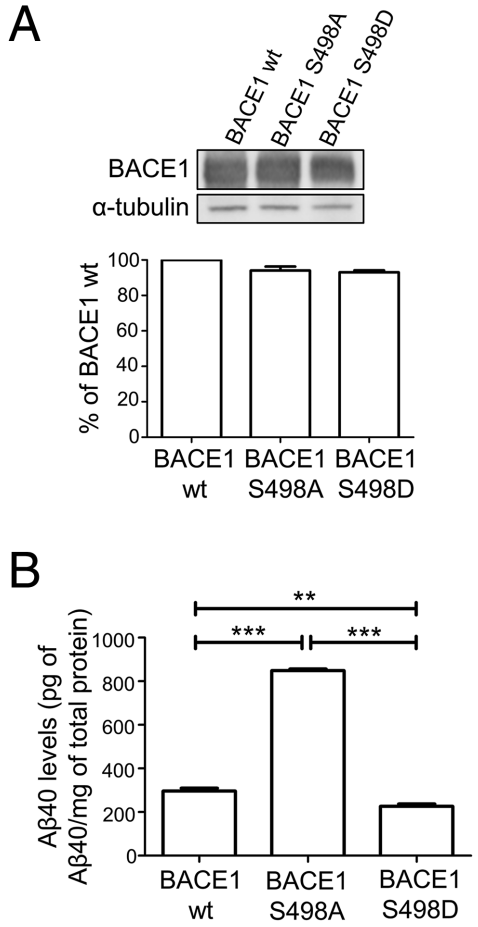

FIGURE 8: BACE1 phosphomutants produce different levels of Aβ peptide. (A) Immunoblotting of cell extracts of CHO cells stably expressing APP_{695wt} and wtBACE1, BACE1 S498A, or BACE1 S498D and probed with rabbit anti-BACE1 antibodies and mouse anti–α-tubulin antibodies, using a chemiluminescence detection system. Bar graph of the densitometric intensity of the BACE1 bands after normalization with density of the α-tubulin bands. Densitometry of the bands was carried out using ImageJ. Data were pooled from three independent experiments and are expressed as the mean ± SEM. (B) Analysis of secreted Aβ in conditioned media of CHO cells stably expressing APP_{695wt} and wtBACE1, BACE1 S498A, or BACE1 S498D using a sandwich ELISA specific for $Aβ_{40}$. The levels of Aβ were normalized against total cell protein and BACE1 expression for each variant. Data are from four independent experiments and expressed as the mean ± SEM. $^{**}p < 0.01$, $^{***}p < 0.001$.

monoclonal antibodies to GGA1 (ab170956), rabbit polyclonal antibodies to Vps26 (ab23892), and mouse antibodies to Vps35 (ab57632) were obtained from Abcam (Cambridge, UK). Monoclonal antibodies to the human transferrin receptor (OKT9) (Schneider *et al.*, 1982) were purified from hydridoma supernatants.

Secondary antibodies used for immunofluorescence were goat anti-rabbit immunoglobulin G (IgG)-Alexa Fluor 568 nm, goat anti-rabbit IgG-Alexa Fluor 488 nm, goat anti-mouse IgG-Alexa Fluor 568 nm, and goat anti-mouse IgG-Alexa Fluor 488 nm, purchased from Life Technologies (Grand Island, NY). Horseradish peroxidase (HRP)-conjugated sheep anti-rabbit Ig and anti-mouse Ig were purchased from DAKO Corporation (Carpinteria, CA).

Generation of antibodies specific for endogenous human BACE1

A peptide corresponding to the N-terminal 35-residue of mature human BACE1 ($BACE1_{1–35}$: PRETDEEPEEPGRRGSFVEMVDNLRGKSGQGYYVEC), with an additional cysteine residue at the C terminus of the peptide, was synthesized (Mimotopes, Victoria, Australia). The sequence of the peptide is 97% identical to the mouse BACE1 N-terminal sequence. The $BACE1_{1–35}$ peptide was injected into New Zealand white rabbits, and two booster injections were given at 28 and 56 d after initial immunization; a terminal bleed was collected at day 66. All immunizations and ELISAs were carried out by Mimotopes (Victoria, Australia). Antibodies from the terminal bleed serum were affinity purified using a column of $BACE1_{1–35}$ peptides coupled to Sulfolink Coupling Gel (Pierce) as per manufacturer's instructions. The specificity of the affinity-purified antibodies was confirmed by immunoblotting and immunofluorescence and reacts with both human and mouse BACE1.

Cell culture and transient transfections

Mycoplasma-free authentic HeLa cells (Curie Institute, Paris) and SK-N-SH cells (American Type Culture Collection, Manassas, VA) were maintained as a semiconfluent monolayer in DMEM supplemented with 10% (vol/vol) fetal calf serum (FCS), 2 nM glutamine, and 100 U/μl penicillin and 0.1% streptomycin (complete DMEM). For transient transfections, HeLa cells were seeded as monolayers in 12-well plates with coverslips. Cells were transfected with plasmid DNA (0.3–1.0 μg/well) using FuGene 6 (Promega) as per manufacturer's protocol.

CHO-APP_{695wt} cell lines stably expressing the wild-type neuronal specific human Amyloid Precursor Protein (APP_{695wt}) isoform were kindly provided by Andrew F. Hill (La Trobe University) (Sharples *et al.*, 2008). The cell lines were maintained in complete-Roswell Park Memorial Institute medium (C-RPMI) supplemented with 7.5 μg/ml puromycin (Invivogen). BACE1wt-APP-CHO, BACE1

system. (B, D) Confocal microscopic images of fixed and permeabilized monolayers stained with rabbit polyclonal anti-human BACE1 antibodies (red) and (B) mouse monoclonal antibodies to Rab11 (green) or (D) mouse monoclonal antibodies to CD63 (green). Higher magnifications of the merge images are shown. Bars represent 10 μm. (C, E) Percentage of BACE1 at the (C) recycling endosomes and (E) late endosomes was calculated from the percentage of total BACE1 pixels that overlapped with Rab11 or CD63, respectively. Data from three independent experiments. (F–I) HeLa cells were transfected with either control siRNA or SNX4 siRNA for 72 h and transfected with the BACE1 S498A (F, G) or BACE1 S498D (H–I) construct for a further 24 h. (F, H) Confocal microscopic images of fixed and permeabilized monolayers stained with rabbit polyclonal anti-human BACE1 antibodies (red) and mouse monoclonal antibodies to Rab11 (green). Higher magnifications of the merge images are shown. Bars represent 10 μm. (G, I) Percentage of (G) BACE1 S498A and (I) BACE1 S498D at the recycling endosomes was calculated from the percentage of total BACE1 pixels that overlapped with Rab11, respectively. Data from three independent experiments.

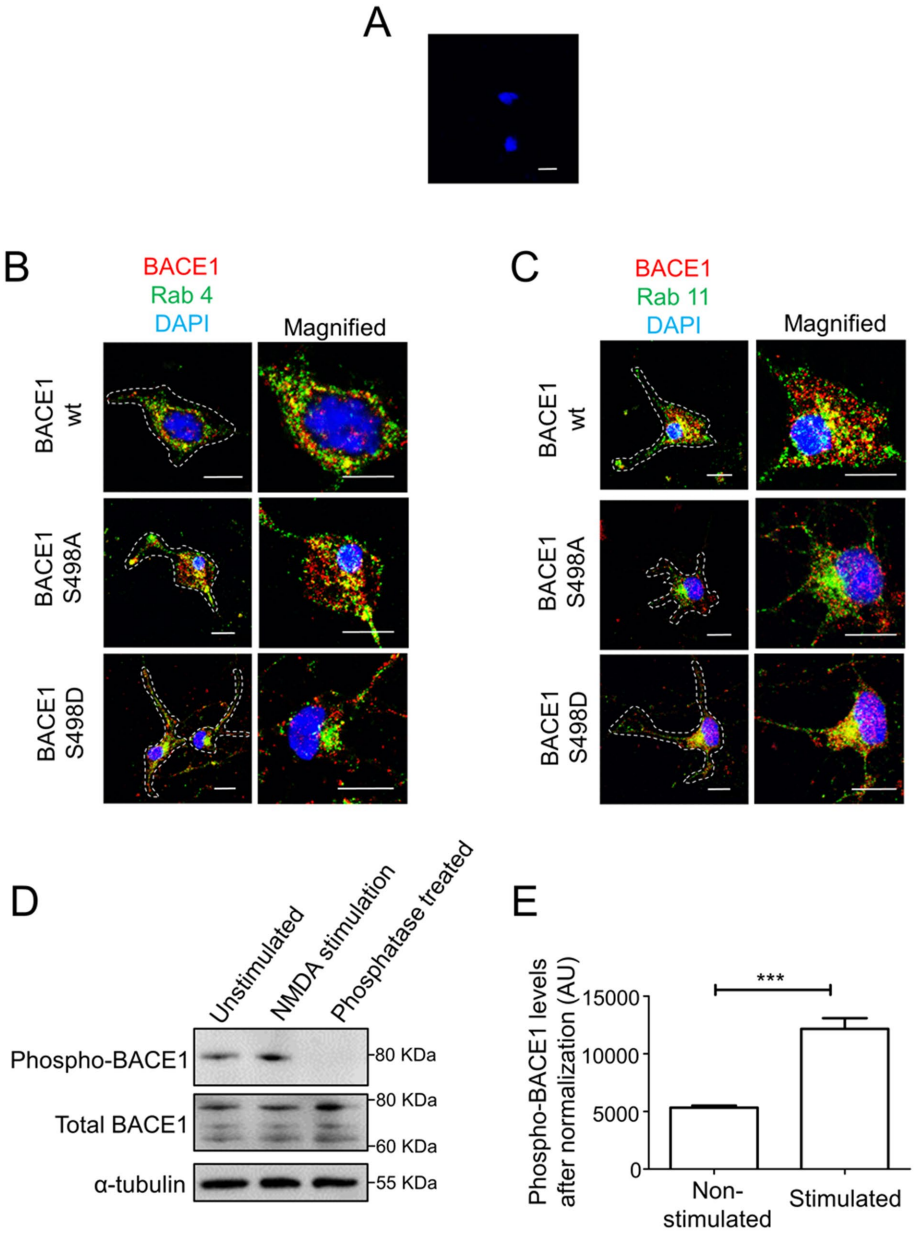

FIGURE 9: Steady distribution of BACE1 phosphomutants in mouse primary embryonic cortical neurons. (A) E16 mouse primary cortical neurons were grown as monolayers for 7 d in culture, fixed, and stained with rabbit polyclonal anti-human BACE1 antibodies (EE-17) and DAPI. (B, C) Confocal images of E16 mouse primary cortical neurons were grown for 7 d in culture and then transfected with either wtBACE1 or BACE1 phosphomutants for 24 h, fixed and permeabilized, and stained with rabbit polyclonal anti-human BACE1 antibodies (EE-17) (red), DAPI, and (B) mouse polyclonal antibodies to Rab4 (green) or (C) mouse monoclonal antibodies to Rab11 (green). Note that the anti-human BACE1 antibodies detect human BACE1 (B, C) but not the mouse endogenous BACE1 (A). (D, E) Immunoblotting of cell extracts of mouse primary cortical neurons grown in culture for 7 d before stimulating with 25 μM NMDA and 25 μM bicuculline. Immunoblot probed with rabbit anti-phosphorylated Ser498 BACE1 antibodies, affinity-purified rabbit polyclonal anti-BACE1 antibodies (laboratory raised), and mouse anti–α-tubulin antibody, using a chemiluminescence detection system. (E) Densitometric quantitation of the phosphoBACE1 bands from (D) normalized to total BACE1 protein in each sample. Data were pooled from three independent experiments and are expressed as mean ± SEM.

S498A-APP-CHO, and BACE1 S498D-APP-CHO cell lines were generated and maintained in C-RPMI (10% [vol/vol] FCS, 2 nM glutamine, and 100 U/μl penicillin and 0.1% streptomycin) supplemented with 7.5 μg/ml puromycin and 50 μg/ml zeocin (Grand Island, NY).

Mouse primary cortical neuronal cultures

All experiments carried out on animals were approved by the Animal Ethics Committee, University of Melbourne (approval number 1212502.1) and in accordance with animal ethics guidelines. Pregnant mice (C57BL/6) at gestational day 15–16 were killed by CO_2 asphyxiation, and the embryos were collected by caesarean section. Embryos collected were used for preparation of the primary cortical neuronal culture. The cortical regions of the embryonic brains, free of meninges, were first aseptically dissected and suspended in Suspension Buffer (250 ml of Hank's balanced salt solution [HBSS; Life Technologies], 1.16 mM $MgSO_4$ [Sigma Aldrich, Australia], 3.0×10^{-3} mg/ml bovine serum albumin [Sigma Aldrich, Australia]). Cortical regions of the brains were pelleted in the centrifuge (1 min, 1000 × *g*). Then the tissue pellet was trypsinized in Trypsin Digestion Buffer (20 ml Suspension Buffer, 0.04 KU/ml DNase [Life Technologies]) containing 0.2 mg/ml trypsin (Sigma Aldrich, Australia) at 37°C for 5 min with shaking. Trypsin digestion was stopped by the addition of Trypsin Inhibitor Buffer (20 ml Suspension Buffer containing 0.83 mg/ml trypsin inhibitor [Sigma Aldrich, Australia], 6.4 KU/μl DNase, and 0.24 mM $MgSO_4$) to the cell suspension before centrifugation for 5 min, 1000 × *g*. The pellet was subjected to mechanical trituration in Trypsin Inhibitor Buffer for 30 s. Trypsinized cells were collected by centrifugation (5 min, 1000 × *g*) and resuspended in neurobasal medium supplemented with 2.5% B-27, 0.25% GlutaMAX, and 100 U/μl penicillin and 0.1% streptomycin (complete NBM) (Life Technologies). Cells were plated at a density of 0.6×10^5 cells/well and 5×10^5 cells/well in 12-well plates and six-well plates, respectively. After 24 h, the medium was replaced with fresh complete NBM. At 5 d in vitro (DIV 5), half of the medium in each well was replaced with fresh complete NBM. Cells were grown for 7 d (DIV 7) before being used for neuronal stimulation treatment, immunoblotting, or immunofluorescence.

Site-directed mutagenesis

The BACE1 LLAA construct was generated using site-directed mutagenesis using primers 5′-TTTGCTGATGACATCTCCGCTGCTAAGTGATGACTCGAGTCT-3′ and 5′-AGACTCGAGTCATCACTTAGCAGCGGAGATGTCATCAGCAAA-3′. The BACE1 S498A construct was generated using site-directed mutagenesis using primers 5′-ATGACTTTGCTGATGATATCGCTCTGCTGAAGTGATGACTCGA-3′ and 5′-TCGAGTCATCACTTCAGCAGAGCGATATCATCAGCAAAGTCAT-3′. The BACE1 S498D construct was generated

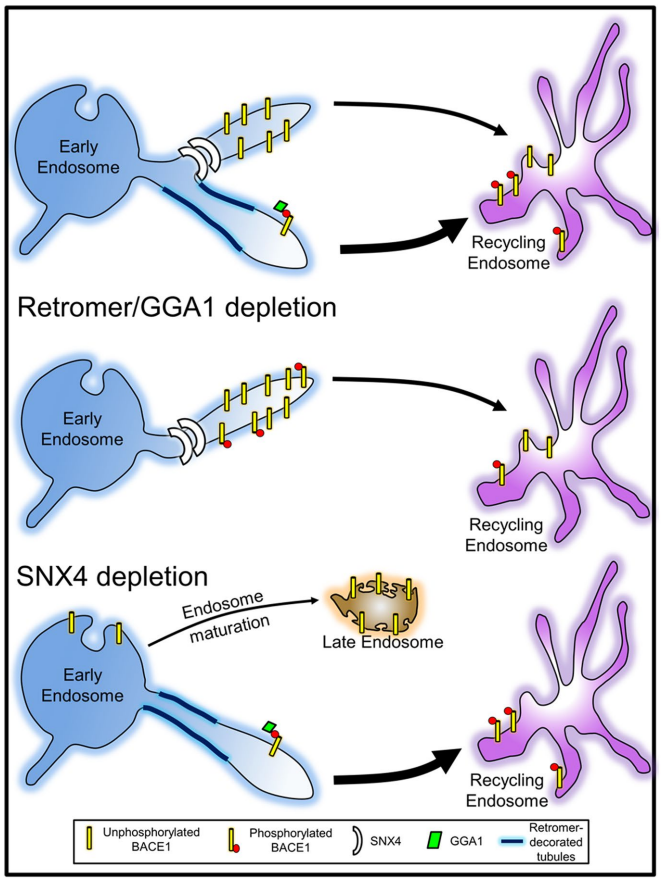

FIGURE 10: Proposed model for endosomal trafficking of BACE1 phosphomutants. After internalization, BACE1 is transported from the early endosomes to the recycling endosomes. Nonphosphorylated BACE1 is transported to the recycling endosomes at a slower rate than phosphorylated BACE1, leading to an extended residency time of nonphosphorylated BACE1 in early endosomes. We propose that nonphosphorylated BACE1 utilizes the SNX4 signal-independent transport pathway to the recycling endosomes, whereas phosphorylated BACE1 is transported by a retromer/GGA1-dependent fast pathway. On retromer/GGA1 depletion, the phosphorylated BACE1 is transported at the same rate as the nonphosphorylated species, and we propose that in the absence of either retromer or GGA1 the phosphorylated and nonphosphorylated species use the same SNX4 pathway to the recycling endosome. Phosphorylated BACE1 is unaffected by the depletion of SNX4.

using site-directed mutagenesis using primers 5′-ATGACTTTG-CTGATGATATCGACCTGCTGAAGTGATGACTCGA-3′ and 5′-TC-GAGTCATCACTTCAGCAGGTCGATATCATCAGCAAAGTCAT-3′. The nucleotide sequence of all mutations and the opening frame was confirmed by DNA sequencing using specific primers: 5′-GAT-CCAGCCTCCGGACTCTA-3′ and 5′-CAGTCGAGGCTGATCAG-CGG-3′.

RNA interference

For siRNA transfections of HeLa cells, monolayers were transfected with siRNA (0.08 μM/well) using Dharmafect 1 (Thermo-Fisher) according to manufacturer's protocol. Transfected cells were incubated for 72 h at 37°C, 10% CO_2. SNX4-specific siRNA duplexes are as described in Traer *et al.* (2007), namely SNX4 siRNA oligonucleotide 1 ACACGAUGACACACAAUAA (indicated throughout as SNX4 siRNA) and oligonucleotide 2 UGGUCAGAGUGUCCUAACA (indicated as SNX4(2) siRNA). Vps26 siRNA is as described in Popoff *et al.* (2009). GGA1 siRNAs are as follows: Oligonucleotide 1 CG-CAACAUCGUGUUCCAGU (indicated throughout as GGA1 siRNA) and oligonucleotide 2 GCAAGUUCCGCUUUCUCAA (indicated as GGA1(2) siRNA). Vps35 siRNA is as follows: AUUUGGUGCGCCU-CAGUCA (Arighi *et al.*, 2004). All duplex siRNAs were manufactured by Sigma-Proligo (Australia).

siRNA-resistant constructs

siRNA-resistant SNX4 was generated by introduction of three silent base mismatches (g147t;a153t;c156t) into the opening reading frame conferring resistance to the SNX4 siRNA oligonucleotide 1 described above. siRNA-resistant GGA1 was generated by introduction of three silent base mismatches (c1677t;c1680t;g1683a) into the opening reading frame conferring resistance to the GGA1 siRNA oligonucleotide 1 described above. siRNA-resistant constructs were synthesized by Genscript. siRNA-resistant Vps26A has been described (Gallon *et al.*, 2014). Rescue experiments were performed by transfection of cell monolayers with siRNAs for 72 h followed by transfection with the siRNA-resistant construct for a further 24 h before cell processing.

Indirect immunofluorescence microscopy

Monolayers on coverslips were fixed in 4% paraformaldehyde (PFA) for 15 min at room temperature (RT), followed by quenching in 50 mM NH_4Cl/phosphate-buffered saline (PBS) for 10 min at room temperature. Cells were permeablized with 0.1% Triton X-100/PBS for 4 min and blocked in Blocking Solution (5% FCS, 0.02% sodium azide in PBS) for 30 min to reduce unspecific binding. For Rab11 and GGA1 staining, cells were fixed with 10% trichoroacetic acid (TCA)/PBS on ice for 15 min, followed by quenching in 30 mM glycine/PBS for 10 min at RT. Cells were permeablized with 0.1% Triton X-100/PBS for 4 min and blocked in Blocking Solution (5% FCS, 0.02% sodium azide in PBS) for 30 min to reduce unspecific binding. Cells were incubated with primary antibodies diluted in blocking solution for 1 h at RT and washed six times in PBS. Diluted fluorochrome-conjugated secondary antibodies were added to cells and incubated for 30 min at RT before being washed six times in PBS. Coverslips were washed in milli-Q water before mounting in Mowoil (10% [wt/vol] Hopval 5–88, 25% [wt/vol] glycerol, 0.1 M Tris in milli-Q water).

Confocal microscopy and image analysis

Confocal microscopy was performed using a Leica TCS SP2 or SP8 system. Images were collected sequentially for multicolor imaging using a ×63/1.4 NA HCX PL APO CS oil immersion objective. GFP and Alexa Fluor488 were excited with the 488-nm line of an argon laser, Alexa Fluor568 with a 543-nm HeNe laser, Alexa Fluor647 with a 633-nm HeNe laser, and 4′,6-diamidine-2′-phenylindole dihydrochloride (DAPI) with a 405-nm UV laser. Images were collected with pixel dimensions of at least 512 × 512. For multicolor labelling, images were collected independently. Three-dimensional reconstructions were generated using the Leica LAS software. Images were cropped in Photoshop.

BACE1 internalization assay

HeLa cells were transfected with pcDNA4/TO BACE1, pcDNA4/TO BACE1 S498D, or pcDNA4/TO BACE1 S498A for 24 h using FuGene 6 (Promega). Monolayers were washed twice with cold PBS before addition of rabbit anti-human BACE1 antibodies (1/400 dilution) and incubated on ice for 30 min. Unbound antibodies were removed by washing twice with cold PBS. Internalization of the antibody-bound BACE1 was carried out in serum-free media at

37°C for the respective time points. Cells at each time point were fixed with either 4% PFA or 10% TCA and the internalized antibody-bound complexes were detected by addition of fluorophore-conjugated secondary antibodies.

Cell-surface expression and pulse-width analysis using flow cytometry

For cell-surface expression studies, live cells were stained in suspension with rabbit anti-BACE1 antibodies for 30 min on ice and fixed with 4% PFA, quenched with 50 mM NH_4Cl, and blocked in Blocking Solution (5% FCS, 0.02% sodium azide in PBS) for 30 min. Antibody-bound complexes were detected by addition of fluorophore-conjugated secondary antibodies. For pulse-width analysis (PulSA) (Toh *et al.*, 2015), cells in suspension were fixed with 4% PFA, quenched with 50 mM NH_4Cl, permeablized with 0.1% Triton X-100 for 4 min in suspension, and blocked in Blocking Solution. Cells were stained with rabbit anti-BACE1 antibodies followed by addition of fluorophore-conjugated secondary antibodies. Cells were analyzed at a medium flow rate in an LSRFortessa flow cytometer, equipped with 405, 488, 561, and 640 nm lasers (BD Biosciences). Approximately 10,000 events were collected, using a forward-scatter threshold of 5000. Data were collected in pulse-height, area, and width parameters for each channel.

Immunoblotting

Equal number of cells were lysed in 4× reducing sample buffer and boiled for 5 min at 100°C. Proteins were resolved on an SDS–PAGE polyacrylamide gel (Life Technologies) and transferred onto Immobilon-P polyvinylidene fluroride membrane (Millipore, NSW, Australia) at 30 V overnight at 4°C. The membrane was blocked by drying at 37°C. The membrane was incubated with primary antibodies diluted in 5% skim milk/PBS for 1 h and then washed three times for 10 min each in 0.1% (vol/vol) PBS-Tween 20. HRP-conjugated secondary antibodies were then added to the membrane for 1 h and washed as above. Bound antibodies were detected using chemiluminescence and captured using the Gel-Pro Analyser version 4.5 software (MediaCybernetics, Bethesda, MD). Densitometry of the protein bands was measured using the Gel-Pro Analyser program. For mouse cortical primary cortical neurons, cells were prepared in RIPA buffer (50 mM Tris-HCl, pH 7.3, 150 mM NaCl, 0.1 mM EDTA, 1% [wt/vol] sodium deoxycholate, 1% [vol/vol] Triton X-100, 0.2% [wt/vol] NaF, and 100 μM Na_3VO_4) supplemented with protease inhibitors. Cell lysates were incubated on ice for 10 min and centrifuged for 10 min at 16,000 × *g*. Protein concentrations were determined by Bradford assay prior to SDS–PAGE.

Aβ ELISA

Secreted $A\beta_{40}$ levels from overnight-conditioned media were measured using an $A\beta_{40}$-specific Aβ ELISA kit (Life Technologies) as per manufacturer's protocol. Secreted Aβ levels were normalized against total protein concentrations of cell lysates as measured using a Bradford assay.

Neuronal stimulation using NMDA

NMDA receptor stimulation was performed on DIV 7 neurons. Neurons were incubated with complete neurobasal medium (NBM) supplemented with 25 μM of NMDA and 25 μM of bicuculline (Sigma-Aldrich, Australia) for 5 min at 37°C. Neurons were washed twice in complete NBM supplemented with 25 μM of bicuculline and subsequently allowed to recover in the above medium for 15 min at 37°C before analysis by immunofluorescence and immunoblotting.

Quantitation of colocalization and statistical analysis

Quantitation of the colocalization between cargo and fluorescent organelle markers was performed using the plug-in organelle-based colocalization (OBCOL) (Woodcroft *et al.*, 2009) on the ImageJ program (National Institutes of Health public domain software). Quantitation was carried out for the indicated number of cells at each time point. For transient transfections, only cells with low-modest expression levels were analyzed. Sample sizes were based on previous studies (Toh *et al.*, 2016) and data shown as dotplots in figures with two and three data sets and bar graphs for figures with more than three data sets. The percentage of cargoes stained with various antibodies at different organelles was calculated by taking the sum of overlapping pixels between the cargo and the different markers divided by the total number of cargo pixels within each cell. All analyses included samples from two or more independent experiments. Data are expressed as the mean ± SEM and were analyzed by an unpaired, two-tailed, Student's *t* test. A $p < 0.05$ (*) was considered significant, $p < 0.01$ (**) was highly significant, and $p < 0.001$ (***) was very highly significant. An absence of a *p* value indicates that the differences were not significant.

ACKNOWLEDGMENTS

Confocal microscopy was performed at the Biological Optical Microscopy Platform (BOMP) at the University of Melbourne. We thank Rohan Teasdale (University of Queenland) and Peter Cullen (University of Bristol) for SNX4 and Vps26A constructs, respectively. This work was supported by funding from the National Health and Medical Research Council (APP1082600). We thank Fiona Houghton for expert technical advice.

REFERENCES

Andersen OM, Reiche J, Schmidt V, Gotthardt M, Spoelgen R, Behlke J, von Arnim CA, Breiderhoff T, Jansen P, Wu X, *et al.* (2005). Neuronal sorting protein-related receptor sorLA/LR11 regulates processing of the amyloid precursor protein. Proc Natl Acad Sci USA 102, 13461–13466.

Arighi CN, Hartnell LM, Aguilar RC, Haft CR, Bonifacino JS (2004). Role of the mammalian retromer in sorting of the cation-independent mannose 6-phosphate receptor. J Cell Biol 165, 123–133.

Balana B, Maslennikov I, Kwiatkowski W, Stern KM, Bahima L, Choe S, Slesinger PA (2011). Mechanism underlying selective regulation of G protein-gated inwardly rectifying potassium channels by the psychostimulant-sensitive sorting nexin 27. Proc Natl Acad Sci USA 108, 5831–5836.

Berman DE, Ringe D, Petsko GA, Small SA (2015). The use of pharmacological retromer chaperones in Alzheimer's disease and other endosomal-related disorders. Neurotherapeutics 12, 12–18.

Bero AW, Yan P, Roh JH, Cirrito JR, Stewart FR, Raichle ME, Lee JM, Holtzman DM (2011). Neuronal activity regulates the regional vulnerability to amyloid-beta deposition. Nat Neurosci 14, 750–756.

Bonifacino JS (2004). The GGA proteins: adaptors on the move. Nat Rev Mol Cell Biol 5, 23–32.

Buggia-Prevot V, Fernandez CG, Riordan S, Vetrivel KS, Roseman J, Waters J, Bindokas VP, Vassar R, Thinakaran G (2014). Axonal BACE1 dynamics and targeting in hippocampal neurons: a role for Rab11 GTPase. Mol Neurodegener 9, 1–17.

Buggia-Prevot V, Fernandez CG, Udayar V, Vetrivel KS, Elie A, Roseman J, Sasse VA, Lefkow M, Meckler X, Bhattacharyya S, *et al.* (2013). A function for EHD family proteins in unidirectional retrograde dendritic transport of BACE1 and Alzheimer's disease Abeta production. Cell Rep 5, 1552–1563.

Burgos PV, Mardones GA, Rojas AL, daSilva LL, Prabhu Y, Hurley JH, Bonifacino JS (2010). Sorting of the Alzheimer's disease amyloid precursor protein mediated by the AP-4 complex. Dev Cell 18, 425–436.

Chia PZ, Ramdzan YM, Houghton FJ, Hatters DM, Gleeson PA (2014). High-throughput quantitation of intracellular trafficking and organelle disruption by flow cytometry. Traffic 15, 572–582.

Chia PZ, Toh WH, Sharples R, Gasnereau I, Hill AF, Gleeson PA (2013). Intracellular itinerary of internalised beta-secretase, BACE1, and its potential impact on beta-amyloid peptide biogenesis. Traffic 14, 997–1013.
Cirrito JR, Yamada KA, Finn MB, Sloviter RS, Bales KR, May PC, Schoepp DD, Paul SM, Mennerick S, Holtzman DM (2005). Synaptic activity regulates interstitial fluid amyloid-beta levels in vivo. Neuron 48, 913–922.
Clairfeuille T, Mas C, Chan AS, Yang Z, Tello-Lafoz M, Chandra M, Widagdo J, Kerr MC, Paul B, Merida I, *et al.* (2016). A molecular code for endosomal recycling of phosphorylated cargos by the SNX27-retromer complex. Nat Struct Mol Biol 23, 921–932.
Collins BM (2008). The structure and function of the retromer protein complex. Traffic 9, 1811–1822.
Cullen PJ, Korswagen HC (2012). Sorting nexins provide diversity for retromer-dependent trafficking events. Nat Cell Biol 14, 29–37.
Danysz W, Parsons CG (2012). Alzheimer's disease, beta-amyloid, glutamate, NMDA receptors and memantine—searching for the connections. Br J Pharmacol 167, 324–352.
Das U, Scott DA, Ganguly A, Koo EH, Tang Y, Roy S (2013). Activity-induced convergence of APP and BACE-1 in acidic microdomains via an endocytosis-dependent pathway. Neuron 79, 447–460.
Das UK, Daifuku SL, Gorelsky SI, Korobkov I, Neidig ML, Le Roy JJ, Murugesu M, Baker RT (2016). Mononuclear, dinuclear, and trinuclear iron complexes featuring a new monoanionic SNS thiolate ligand. Inorg Chem 55, 987–997.
Finan GM, Okada H, Kim TW (2011). BACE1 retrograde trafficking is uniquely regulated by the cytoplasmic domain of sortilin. J Biol Chem 286, 12602–12616.
Gallon M, Clairfeuille T, Steinberg F, Mas C, Ghai R, Sessions RB, Teasdale RD, Collins BM, Cullen PJ (2014). A unique PDZ domain and arrestin-like fold interaction reveals mechanistic details of endocytic recycling by SNX27-retromer. Proc Natl Acad Sci USA 111, E3604–E3613.
Gallon M, Cullen PJ (2015). Retromer and sorting nexins in endosomal sorting. Biochem Soc Trans 43, 33–47.
Ghai R, Bugarcic A, Liu H, Norwood SJ, Skeldal S, Coulson EJ, Li SS, Teasdale RD, Collins BM (2013). Structural basis for endosomal trafficking of diverse transmembrane cargos by PX-FERM proteins. Proc Natl Acad Sci USA 110, E643–E652.
Ginsberg SD, Mufson EJ, Alldred MJ, Counts SE, Wuu J, Nixon RA, Che S (2011). Upregulation of select rab GTPases in cholinergic basal forebrain neurons in mild cognitive impairment and Alzheimer's disease. J Chem Neuroanat 42, 102–110.
Grant BD, Donaldson JG (2009). Pathways and mechanisms of endocytic recycling. Nat Rev Mol Cell Biol 10, 597–608.
He X, Li F, Chang WP, Tang J (2005). GGA proteins mediate the recycling pathway of memapsin 2 (BACE). J Biol Chem 280, 11696–11703.
Herskowitz JH, Offe K, Deshpande A, Kahn RA, Levey AI, Lah JJ (2012). GGA1-mediated endocytic traffic of LR11/SorLA alters APP intracellular distribution and amyloid-beta production. Mol Biol Cell 23, 2645–2657.
Hsu VW, Bai M, Li J (2012). Getting active: protein sorting in endocytic recycling. Nat Rev Mol Cell Biol 13, 323–328.
Hsu VW, Prekeris R (2010). Transport at the recycling endosome. Curr Opin Cell Biol 22, 528–534.
Huse JT, Pijak DS, Leslie GJ, Lee VM, Doms RW (2000). Maturation and endosomal targeting of beta-site amyloid precursor protein-cleaving enzyme. The Alzheimer's disease beta-secretase. J Biol Chem 275, 33729–33737.
Kamenetz F, Tomita T, Hsieh H, Seabrook G, Borchelt D, Iwatsubo T, Sisodia S, Malinow R (2003). APP processing and synaptic function. Neuron 37, 925–937.
Kang EL, Cameron AN, Piazza F, Walker KR, Tesco G (2010). Ubiquitin regulates GGA3-mediated degradation of BACE1. J Biol Chem 285, 24108–24119.
Kim NY, Cho MH, Won SH, Kang HJ, Yoon SY, Kim DH (2017). Sorting nexin-4 regulates beta-amyloid production by modulating beta-site-activating cleavage enzyme-1. Alzheimers Res Ther 9, 4.
Kinoshita A, Fukumoto H, Shah T, Whelan CM, Irizarry MC, Hyman BT (2003). Demonstration by FRET of BACE interaction with the amyloid precursor protein at the cell surface and in early endosomes. J Cell Sci 116, 3339–3346.
Koo EH, Squazzo SL, Selkoe DJ, Koo CH (1996). Trafficking of cell-surface amyloid beta-protein precursor. I. Secretion, endocytosis and recycling as detected by labeled monoclonal antibody. J Cell Sci 109(Pt 5), 991–998.
Lieu ZZ, Gleeson PA (2011). Endosome-to-Golgi transport pathways in physiological processes. Histol Histopathol 26, 395–408.
Lim JP, Teasdale RD, Gleeson PA (2012). SNX5 is essential for efficient macropinocytosis and antigen processing in primary macrophages. Biol Open 1, 904–914.
Lorenzen A, Samosh J, Vandewark K, Anborgh PH, Seah C, Magalhaes AC, Cregan SP, Ferguson SS, Pasternak SH (2010). Rapid and direct transport of cell surface APP to the lysosome defines a novel selective pathway. Mol Brain 3, 11.
McKenzie JE, Raisley B, Zhou X, Naslavsky N, Taguchi T, Caplan S, Sheff D (2012). Retromer guides STxB and CD8-M6PR from early to recycling endosomes, EHD1 guides STxB from recycling endosome to Golgi. Traffic 13, 1140–1159.
Mecozzi VJ, Berman DE, Simoes S, Vetanovetz C, Awal MR, Patel VM, Schneider RT, Petsko GA, Ringe D, Small SA (2014). Pharmacological chaperones stabilize retromer to limit APP processing. Nat Chem Biol 10, 443–449.
Muhammad A, Flores I, Zhang H, Yu R, Staniszewski A, Planel E, Herman M, Ho L, Kreber R, Honig LS, *et al.* (2008). Retromer deficiency observed in Alzheimer's disease causes hippocampal dysfunction, neurodegeneration, and Abeta accumulation. Proc Natl Acad Sci USA 105, 7327–7332.
Oishi M, Nairn AC, Czernik AJ, Lim GS, Isohara T, Gandy SE, Greengard P, Suzuki T (1997). The cytoplasmic domain of Alzheimer's amyloid precursor protein is phosphorylated at Thr654, Ser655, and Thr668 in adult rat brain and cultured cells. Mol Med 3, 111–123.
Pastorino L, Ikin AF, Nairn AC, Pursnani A, Buxbaum JD (2002). The carboxyl-terminus of BACE contains a sorting signal that regulates BACE trafficking but not the formation of total A(beta). Mol Cell Neurosci 19, 175–185.
Peric A, Annaert W (2015). Early etiology of Alzheimer's disease: tipping the balance toward autophagy or endosomal dysfunction? Acta Neuropathol 129, 363–381.
Popoff V, Mardones GA, Bai SK, Chambon V, Tenza D, Burgos PV, Shi A, Benaroch P, Urbe S, Lamaze C, *et al.* (2009). Analysis of articulation between clathrin and retromer in retrograde sorting on early endosomes. Traffic 10, 1868–1880.
Popoff V, Mardones GA, Tenza D, Rojas R, Lamaze C, Bonifacino JS, Raposo G, Johannes L (2007). The retromer complex and clathrin define an early endosomal retrograde exit site. J Cell Sci 120, 2022–2031.
Prabhu Y, Burgos PV, Schindler C, Farias GG, Magadan JG, Bonifacino JS (2012). Adaptor protein 2-mediated endocytosis of the beta-secretase BACE1 is dispensable for amyloid precursor protein processing. Mol Biol Cell 23, 2339–2351.
Puertollano R, Bonifacino JS (2004). Interactions of GGA3 with the ubiquitin sorting machinery. Nat Cell Biol 6, 244–251.
Rajendran L, Honsho M, Zahn TR, Keller P, Geiger KD, Verkade P, Simons K (2006). Alzheimer's disease beta-amyloid peptides are released in association with exosomes. Proc Natl Acad Sci USA 103, 11172–11177.
Rajendran L, Knolker HJ, Simons K (2010). Subcellular targeting strategies for drug design and delivery. Nat Rev Drug Discov 9, 29–42.
Ramdzan YM, Polling S, Chia CP, Ng IH, Ormsby AR, Croft NP, Purcell AW, Bogoyevitch MA, Ng DC, Gleeson PA, Hatters DM (2012). Tracking protein aggregation and mislocalization in cells with flow cytometry. Nat Methods 9, 467–470.
Ren M, Xu G, Zeng J, De Lemos-Chiarandini C, Adesnik M, Sabatini DD (1998). Hydrolysis of GTP on rab11 is required for the direct delivery of transferrin from the pericentriolar recycling compartment to the cell surface but not from sorting endosomes. Proc Natl Acad Sci USA 95, 6187–6192.
Rogaeva E, Meng Y, Lee JH, Gu Y, Kawarai T, Zou F, Katayama T, Baldwin CT, Cheng R, Hasegawa H, *et al.* (2007). The neuronal sortilin-related receptor SORL1 is genetically associated with Alzheimer disease. Nat Genet 39, 168–177.
Scherzer CR, Offe K, Gearing M, Rees HD, Fang G, Heilman CJ, Schaller C, Bujo H, Levey AI, Lah JJ (2004). Loss of apolipoprotein E receptor LR11 in Alzheimer disease. Arch Neurol 61, 1200–1205.
Schneider C, Sutherland R, Newman R, Greaves M (1982). Structural features of the cell surface receptor for transferrin that is recognized by the monoclonal antibody OKT9. J Biol Chem 257, 8516–8522.
Seaman MN (2007). Identification of a novel conserved sorting motif required for retromer-mediated endosome-to-TGN retrieval. J Cell Sci 120, 2378–2389.
Sharples RA, Vella LJ, Nisbet RM, Naylor R, Perez K, Barnham KJ, Masters CL, Hill AF (2008). Inhibition of gamma-secretase causes increased secretion of amyloid precursor protein C-terminal fragments in association with exosomes. FASEB J 22, 1469–1478.

Shiba T, Kametaka S, Kawasaki M, Shibata M, Waguri S, Uchiyama Y, Wakatsuki S (2004). Insights into the phosphoregulation of beta-secretase sorting signal by the VHS domain of GGA1. Traffic 5, 437–448.
Siegenthaler BM, Rajendran L (2012). Retromers in Alzheimer's disease. Neurodegener Dis 10, 116–121.
Small SA, Gandy S (2006). Sorting through the cell biology of Alzheimer's disease: intracellular pathways to pathogenesis. Neuron 52, 15–31.
Small SA, Kent K, Pierce A, Leung C, Kang MS, Okada H, Honig L, Vonsattel JP, Kim TW (2005). Model-guided microarray implicates the retromer complex in Alzheimer's disease. Ann Neurol 58, 909–919.
Small SA, Petsko GA (2015). Retromer in Alzheimer disease, Parkinson disease and other neurological disorders. Nat Rev Neurosci 16, 126–132.
Sullivan CP, Jay AG, Stack EC, Pakaluk M, Wadlinger E, Fine RE, Wells JM, Morin PJ (2011). Retromer disruption promotes amyloidogenic APP processing. Neurobiol Dis 43, 338–345.
Tesco G, Koh YH, Kang EL, Cameron AN, Das S, Sena-Esteves M, Hiltunen M, Yang SH, Zhong Z, Shen Y, *et al*. (2007). Depletion of GGA3 stabilizes BACE and enhances beta-secretase activity. Neuron 54, 721–737.
Toh WH, Gleeson PA (2016). Dysregulation of intracellular trafficking and endosomal sorting in Alzheimer's disease: controversies and unanswered questions. Biochem J 473, 1977–1993.
Toh WH, Houghton FJ, Chia PZ, Ramdzan YM, Hatters DM, Gleeson PA (2015). Application of flow cytometry to analyze intracellular location and trafficking of cargo in cell populations. Methods Mol Biol 1270, 227–238.
Toh WH, Tan JZ, Zulkefli KL, Houghton FJ, Gleeson PA (2016). Amyloid precursor protein traffics from the Golgi directly to early endosomes in an Arl5b- and AP4-dependent pathway. Traffic 18, 159–175.
Traer CJ, Rutherford AC, Palmer KJ, Wassmer T, Oakley J, Attar N, Carlton JG, Kremerskothen J, Stephens DJ, Cullen PJ (2007). SNX4 coordinates endosomal sorting of TfnR with dynein-mediated transport into the endocytic recycling compartment. Nat Cell Biol 9, 1370–1380.
Udayar V, Buggia-Prevot V, Guerreiro RL, Siegel G, Rambabu N, Soohoo AL, Ponnusamy M, Siegenthaler B, Bali J, Aesg, Simons M, *et al*. (2013). A paired RNAi and RabGAP overexpression screen identifies Rab11 as a regulator of beta-amyloid production. Cell Rep 5, 1536–1551.
Ullrich O, Reinsch S, Urbe S, Zerial M, Parton RG (1996). Rab11 regulates recycling through the pericentriolar recycling endosome. J Cell Biol 135, 913–924.
van Ijzendoorn SC (2006). Recycling endosomes. J Cell Sci Suppl 119, 1679–1681.
van Weering JR, Cullen PJ (2014). Membrane-associated cargo recycling by tubule-based endosomal sorting. Semin Cell Dev Biol 31, 40–47.
Vardarajan BN, Bruesegem SY, Harbour ME, Inzelberg R, Friedland R, St George-Hyslop P, Seaman MN, Farrer LA (2012). Identification of Alzheimer disease-associated variants in genes that regulate retromer function. Neurobiol Aging 33, 2215–2231.
Vieira SI, Rebelo S, Domingues SC, da Cruz e Silva EF, da Cruz e Silva OA (2009). S655 phosphorylation enhances APP secretory traffic. Mol Cell Biochem 328, 145–154.
Vieira SI, Rebelo S, Esselmann H, Wiltfang J, Lah J, Lane R, Small SA, Gandy S, da Cruz ESEF, da Cruz ESOA (2010). Retrieval of the Alzheimer's amyloid precursor protein from the endosome to the TGN is S655 phosphorylation state-dependent and retromer-mediated. Mol Neurodegener 5, 40.
von Arnim CAF, Tangredi MM, Peltan ID, Lee BM, Irizarry MC, Kinoshita A, Hyman BT (2004). Demonstration of BACE ({beta}-secretase) phosphorylation and its interaction with GGA1 in cells by fluorescence-lifetime imaging microscopy. J Cell Sci 117, 5437–5445.
Wahle T, Prager K, Raffler N, Haass C, Famulok M, Walter J (2005). GGA proteins regulate retrograde transport of BACE1 from endosomes to the trans-Golgi network. Mol Cell Neurosci 29, 453–461.
Walter J, Fluhrer R, Hartung B, Willem M, Kaether C, Capell A, Lammich S, Multhaup G, Haass C (2001). Phosphorylation regulates intracellular trafficking of beta-secretase. J Biol Chem 276, 14634–14641.
Wang X, Huang T, Bu G, Xu H (2014). Dysregulation of protein trafficking in neurodegeneration. Mol Neurodegener 9, 31.
Wassmer T, Attar N, Harterink M, van Weering JR, Traer CJ, Oakley J, Goud B, Stephens DJ, Verkade P, Korswagen HC, Cullen PJ (2009). The retromer coat complex coordinates endosomal sorting and dynein-mediated transport, with carrier recognition by the trans-Golgi network. Dev Cell 17, 110–122.
Wen L, Tang FL, Hong Y, Luo SW, Wang CL, He W, Shen C, Jung JU, Xiong F, Lee DH, *et al*. (2011). VPS35 haploinsufficiency increases Alzheimer's disease neuropathology. J Cell Biol 195, 765–779.
Wersto RP, Chrest FJ, Leary JF, Morris C, Stetler-Stevenson MA, Gabrielson E (2001). Doublet discrimination in DNA cell-cycle analysis. Cytometry 46, 296–306.
Woodcroft BJ, Hammond L, Stow JL, Hamilton NA (2009). Automated organelle-based colocalization in whole-cell imaging. Cytometry A 75, 941–950.